The Role of ERK/MAPK In The Postnatal Development of Lower Motor Neurons

by

Colton Dane Smith

A Thesis Presented in Partial Fulfillment
of the Requirements for the Degree
Master of Science

Approved July 2017 by the
Graduate Supervisory Committee

Jason Newbern, Chair
Janet Neisewander
Thomas Hamm

ARIZONA STATE UNIVERSITY

August 2017

ABSTACT

The Erk/MAPK pathway plays a major role in cell growth, differentiation, and survival. Genetic mutations that cause dysregulation in this pathway can result in the development of Rasopathies, a group of several different syndromes including Noonan Syndrome, Costello Syndrome, and Neurofibromatosis Type-1. Since these mutations are germline and affect all cell types it is hard to differentiate the role that Erk/MAPK plays in each cell type. Previous research has shown that individual cell types utilize the Erk/MAPK pathway in different ways. For example, the morphological development of lower motor neuron axonal projections is Erk/MAPK-independent during embryogenesis, while nociceptive neuron projections require ERK/MAPK to innervate epidermal targets. Here, we tested whether Erk/MAPK played a role in the postnatal development of lower motor neurons during crucial periods of activity-dependent circuit modifications. We have generated Cre-dependent conditional Erk/MAPK mutant mice that exhibit either loss or gain of Erk/MAPK signaling specifically in ChAT:Cre expressing lower motor neurons. Importantly, we found that Erk/MAPK is necessary for the development of neuromuscular junction morphology by the second postnatal week. In contrast, we were unable to detect a significant difference in lower motor neuron development in Erk/MAPK gain-of-function mice. The data suggests that Erk/MAPK plays an important role in postnatal lower motor neuron development by regulating the morphological maturation of the neuromuscular junction.

TABLE OF CONTENTS

CHAPTER Page

CHAPTER Page

CHAPTER Page

LIST OF FIGURES

FIGURE Page

FIGURE Page

CHAPTER I LITERATURE REVIEW

Role of Kinases During Development

During development, intercellular communication is crucial for the regulation of proper cellular differentiation and function. Cells accomplish this in part via extracellular polypeptide ligands that act upon receptors expressed on the cell membrane (Hubbard and Till, 2000). One prominent class of receptors, receptor tyrosine kinases (RTKs), are transmembrane glycoproteins that bind specific ligands and function to transduce extracellular signals that regulate cell development including proliferation, migration, and/or differentiation (Schlessinger and Ullrich, 1992). RTKs activate a number of intracellular signaling cascades that mediate a wide range of cellular behaviors including PI3-Kinase, PLCgamma, and ERK/Mitogen-activated protein kinases (Erk/MAPK). Erk/MAPKs are a highly conserved pathway that features a sequential three-tier structure consisting of Raf (ARAF, BRAF, CRAF), Mek (MEK1 & MEK2), and Erk (ERK1 & ERK2) (Krishna and Narang, 2008). The individual tiers of the MAP Kinase pathway are phosphorylated, and thus activated, by upstream Ras/Rho family proteins that are activated by a range of external signals (Krishna and Narang, 2008). In the Erk/MAPK signaling pathway activated Ras leads to the phosphorylation of B/C-Raf, which in turns phosphorylates MEK1/2, which then phosphorylates ERK1/2. The end of this three-tier pathway features MAPK binding to specific targets, phosphorylating them, and activating substrates such as transcription factors and protein kinases (Nishimoto and Nishida, 2006). Simply put, extracellular signals bind to the surface of the cell and triggers

biochemical mechanisms that alter cellular behavior.

Four main types of MAPK signaling cascades can be found in mammals. These are the extracellular signal regulated kinases 1 and 2 (ERK1/2 or Erk/MAPK), extracellular signal regulated kinase 5 (ERK5), c-Jun N-terminal kinase (JNK), and P38 (Newbern et al. 2011; Rauen, 2013). In the context of neurodevelopment ERK1/2 and ERK5 are important MAPK pathways due to their role in the regulation of cell proliferation and differentiation (Nishimoto and Nishida, 2006). Both pathways respond to similar trophic stimuli, such as nerve growth factor (NGF), and can also induce immediate early genes, such as c-fos and c-jun (Kamakura *et al*, 1999; Kato et al, 1997).

Rasopathies

The Erk/MAPK pathway has been extensively studied in the context of both cancer and development. Oncogenesis research has discovered that about 20% of cancer cases have a mutation in Ras and around 7% have a mutation in BRaf (Bos, 1989; Pritchard et al, 2007). Given the role of MAPK pathways in the proliferation of cells it makes sense that mutations in components of this pathway could lead to unregulated cell proliferation. Research is also being done to understand the effects of genetic mutations in Erk/MAPK signaling in the context of developmental biology. Developmental disorders known as Rasopathies contain germline mutations in genes that regulate Erk/MAPK signaling which can cause profound effects on the development of an

organism due to the organism's early reliance on extracellular input to induce cell proliferation and differentiation (Rauen, 2013).

Rasopathies are typically characterized by cutaneous abnormalities, musculoskeletal defects, cardiac issues, neurological problems, and a predisposition to various forms of cancer (Stevenson, 2012; Rauen, 2013). Patients with NF1, Costello syndrome, and cardio-facio cutaneous syndrome share common muscular phenotypes such as hypotonia and variable muscle fiber size (Tidyman et al., 2011). This results in weakness, gross motor delays, hypotonia, and underdeveloped muscle bulk (Tidyman et al., 2011). Patients with NF1 have been shown to have abnormal motor proficiency (Souza et al., 2009), weakness (Johnson et al., 2011), and decreased muscle area (Stevenson et al., 2005). Tests like the one-legged vertical jump test and hand-held dynamometry reveal a significant reduction in force production from NF1 patients (Viskochil et al., 2013). Patients with CFC syndrome have hypertonia and dysfunctional gait (Reinker et al., 2011). Reports of weakness and an increased density of muscle spindles have been found in individuals with Costello Syndrome and Noonan syndrome (van der Burgt et al., 2007). These data clearly indicate that the neuromuscular system does not develop correctly in Rasopathies. However, whether deficits are driven by problems in the muscle, the nervous system, or both is not well understood.

Motor Neurons

There are two main motor neuron types that regulate muscle movement; upper motor neurons and lower motor neurons. The upper motor neurons originate in the motor

cortex and send their axons down the spinal cord where they synapse onto lower motor neurons. These lower motor neurons, also known as spinal motor neurons, are located into the ventral horn of the spinal cord and are found in the most rostral level of the spinal cord all the way down to the most caudal level. Lower motor neurons are specialized cell types that extend their axons out to the periphery, synapse onto muscle fibers, and ultimately function to initiate muscle contraction and movement.

Among these lower motor neurons are several subtypes that perform different functions including alpha, beta, and gamma motor neurons (Figure 1). Alpha motor neurons innervate large extrafusal muscle fibers and are responsible for muscular contraction. They are the characterized by a large cell body and their characteristic neuromuscular junctions. This subtype of motor neuron can be further subdivided into three categories depending on the type of extrafusal muscle fiber they innervate: slow-twitch fatigue-resistant (SFR), fast-twitch fatigue-resistant (FFR), and fast-twitch fatigable (FF) (Burke et al, 1973). SFR lower motor neurons are the first to fire during muscular contraction. This is due to their higher input-resistance, a result of having a smaller cell body, which causes them to respond to a lower threshold of stimulation. FFR lower motor neurons fire second during muscular contraction. This is due to having lower input-resistance than SFR neurons and having higher input-resistance than FF neurons. FF lower motor neurons are the final subtype to fire during muscular contraction. They fire slowly due to having a large cell body and therefore lower input-resistance. The recruitment order of these neurons, from smallest to largest, during muscular contraction is the known as the “size principal” (Mendell, 2005). The differing properties of the alpha

motor neurons subtypes lead to different mean conduction velocities: 100m/s for FF and 85m/s for SFR (Burke et al, 1973).

Beta motor neurons innervate both extrafusal and intrafusal muscle fibers (Bessou, Emonet-Denand, & Laporte, 1965). This allows them to contract muscle and provide sensory feedback from muscle spindles. They can be further divided into two subtypes: static and dynamic. Static beta motor neurons innervate nuclear chain fibers and work to increase the firing rate of type Ia and II sensory fibers. Dynamic beta motor neurons innervate muscle spindle bag fibers and work to increase the stretch sensitivity of type Ia sensory fibers. Given their small size and lower abundance these motor neurons are not as well understood as the other subtypes of lower motor neurons.

Gamma motor neurons modulate the sensitivity of muscle spindles within muscle fibers. They can be further subdivided into two subtypes: static and dynamic. Static gamma motor neurons innervate nuclear chain fibers and static nuclear bag fibers. Dynamic gamma motor neurons innervate dynamic nuclear chain fibers. Though the two subtypes of gamma motor neurons innervate different targets they both work to adjust the sensitivity of muscle spindles by keeping them taut. The coordinated effort between th sensory information coming from the muscle spindle and the motor information being sent to the muscle spindle allows the continued firing of alpha motor neurons and is important for maintaining proper sensory function of spindles during contraction (Kandel et al., 2015)

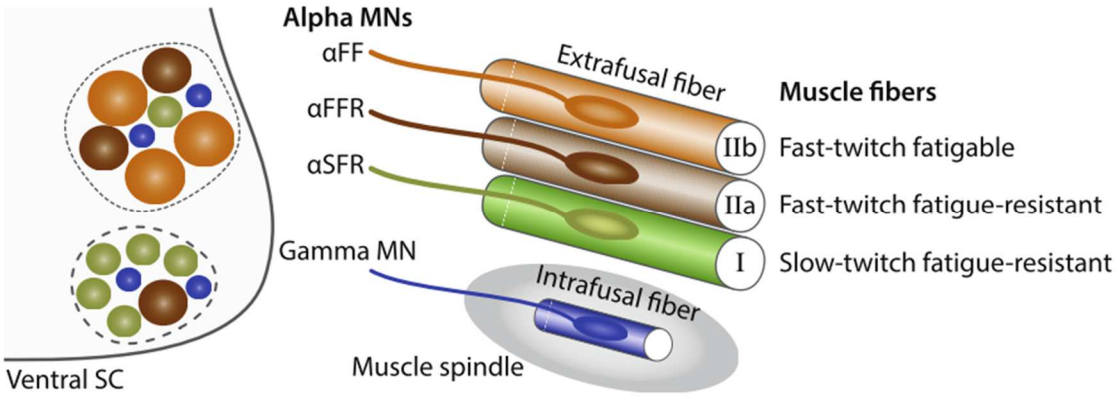

Figure 1: Motor Neuron Subtypes (Stifani, 2014) The three types of alpha motor neurons are alpha fast fatigable (aFF), alpha fast-twitch fatigue-resistant (aFFR), and alpha slow-twitch fatigue-resistant (aSFR). These alpha motor neurons innervate fast-twitch fatigable, fast-twitch fatigue-resistant, and slow-twitch fatigue-resistant muscle fibers. The gamma motor neuron is another subclass of motor neuron. It innervates the intrafusal bag fibers of muscle spindles.

Lower Motor Neuron Development

The development of lower motor neurons begins when the ectoderm undergoes neurulation shortly after gastrulation. During neurulation, the ectoderm folds into itself and leads to the formation of the neural tube, neural crest cells, and the external ectoderm (Figure 2A-2C). From the neural tube emerges the entire CNS (Purves et al, 2011). After neurulation, the neural tube begins to differentiate even further into specialized spinal cord progenitor domains (Figure 2D). This is accomplished by several inductive signals that surround the neural tube.

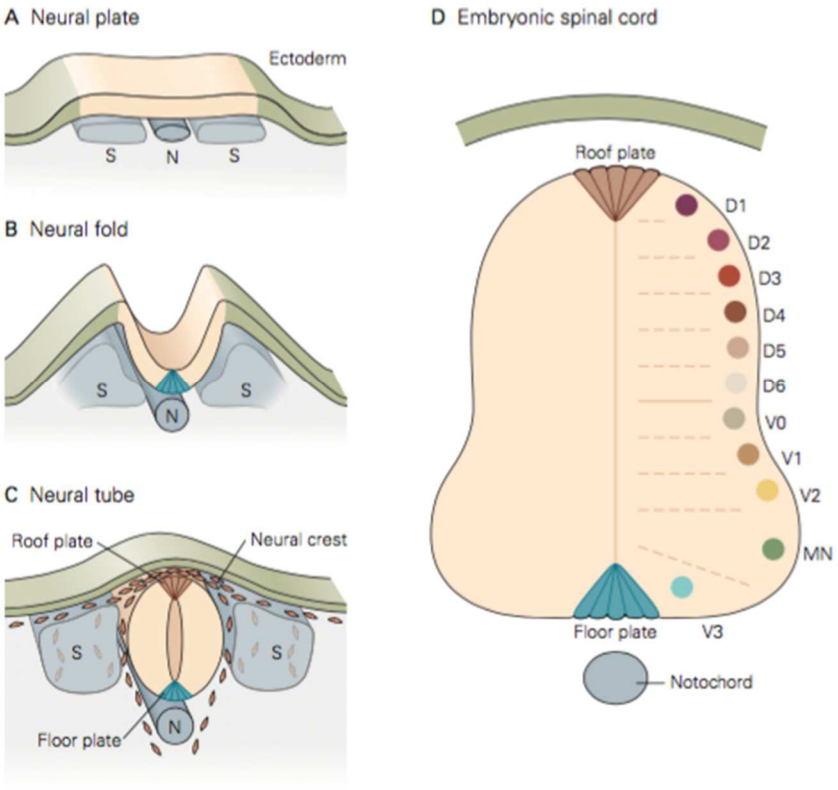

Figure 2: Early Embryogenesis and Embryonic Spinal Cord. (A-C) Schematic of the process of neurulation (D) Schematic of the dorsoventral axis of neuronal subtypes. (adapted from Kandel, 2013)

Dorsoventral Patterning

The dorsoventral patterning of the spinal cord arises from inductive factors secreted from the overlying roof plate and ectoderm and the underlying floor plate and notochord. The roof plate and ectoderm secrete the inductive signals wingless-related integration site proteins (WNTs) and bone morphogenic proteins (BMPs) to establish a decreasing dorsal to ventral gradient (A. Liu & Niswander, 2005). The floorplate and

notochord secrete sonic hedgehog morphogen (SHH) to establish an increasing dorsal to ventral gradient (Briscoe & Ericson, 2001). These dorsoventral inductive signal gradients collaborate to repress different homeodomain transcription factors to generate unique neuronal progenitor domains (Figure 3). These ventral progenitor domains give rise to the lower motor neurons and the surrounding interneuron populations.

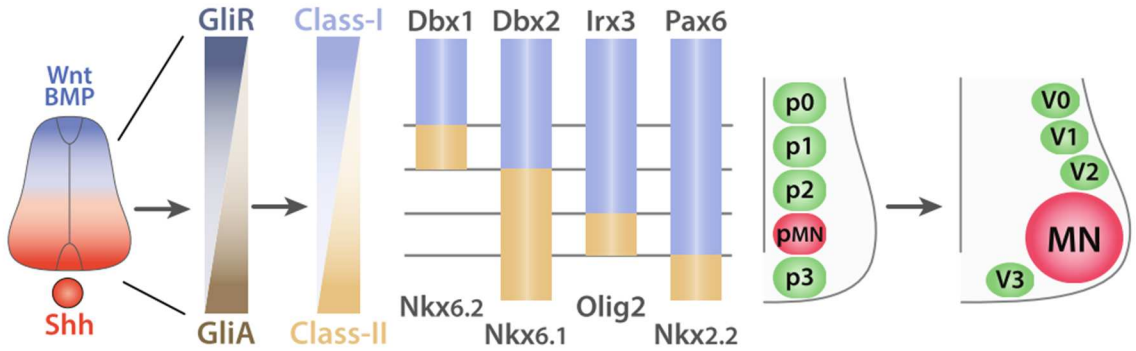

Figure 3: Generation of The Ventral Spinal Cord Progenitor Domains.
Schematic of the process by which inductive signals surrounding the spinal cord work to repress homeodomain transcription factors and form individual domains of neurons. (adapted from Stifani, 2014)

Lower Motor Neuron Specification

Once the motor neuron progenitor domain has been established, further specification of motor neurons begins. The motor neurons of the spinal cord can be characterized in many different ways, including their position along the rostro-caudal axis, the specific muscle they innervate, which spinal column they're found in, and whether they project to the dorsal or ventral side of the body (Dasen & Jessell, 2009). The positional identity of each motor neuron on the rostrocaudal axis is determined by

the coordinative effort of multiple molecular inducers. High levels of retinoic acid (RA) promote the differentiation of rostral motor neurons in the cervical and brachial region while a high level of FGF8 and Gdf11 promote the differentiation of caudal motor neurons in the thoracic and lumbar regions (J.-P. Liu, Laufer, & Jessell, 2001) (Figure 4).

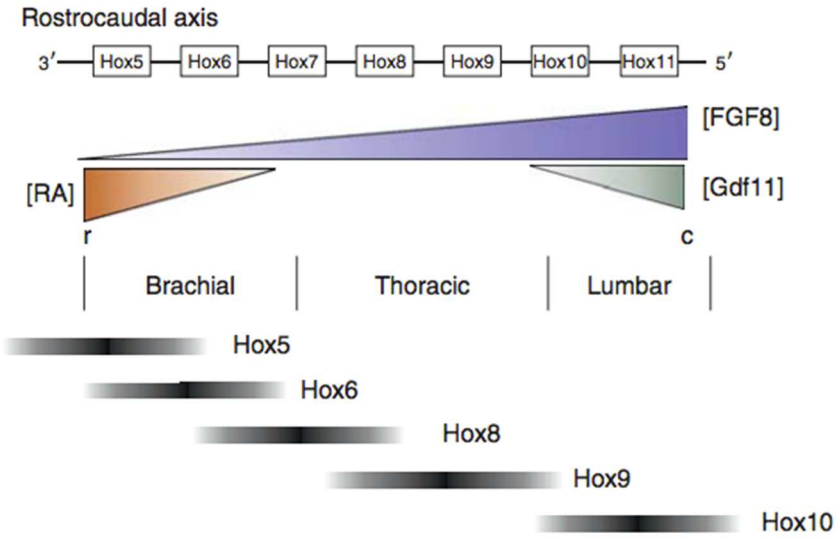

Figure 4: Rostrocaudal Inductive Factors. Schematic of the inductive factors, e.g. RA and FGF8, and their rostrocaudal expression (Dasen & Jessell, 2009)

The molecules that establish the rostocaudal gradient and induce the specification of neuronal subtype identity are integrated by Hox transcription factors (Dasen & Jessell, 2009) (Figure 5). In both the mouse and human, the Hox genes can be found on four chromosomal clusters that have spatial organization based on where they are expressed in the embryo. Hox genes that are closer to the 3' end of the chromosome, like Hox5, are expressed at brachial levels whereas Hox genes closer to the 5' end of the chromosome, like Hox11, are expressed at lumbar levels (Lappin, Grier, Thompson, & Halliday, 2006).

The specific spatial expression of different Hox genes within the spinal cord work to establish motor neuron pool identity and specify the type of muscle that it will eventually innervate (Dasen et al., 2005).

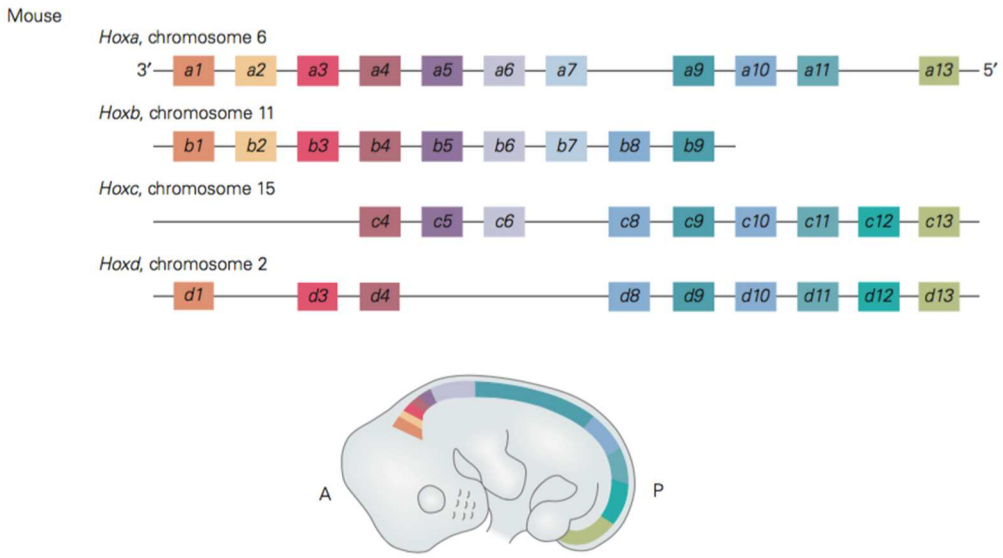

Figure 5: Vertebrate Hox Gene Clusters

Schematic of the four chromosomal Hox gene clusters in the mouse (adapted from Kandel, 2013)

Axon Guidance and Synaptogenesis

Before the motor neuron can exert any control over movement, three cells need to travel long distances. The first cell types are myogenic precursors that eventually form the muscle. Myogenic precursors from the mesoderm travel to the sites where muscles will form, differentiate into myoblasts, and subsequently fuse into myotubes (Buckingham et al., 2003) (Figure 6a-b). The myotubes line up in parallel and become

the muscle fibers with which neurons will synapse on to. The second cell types are the lower motor neurons. The lower motor neurons must send their axons out into the periphery in order to synapse onto muscle fibers (Figure 6a-e). This process is called axonal guidance and there is a rich panoply of molecular mechanisms that guide the axon on its long journey (Tessier-Lavigne & Goodman, 1996). The third cell types that must make their journey into the periphery are myelinating glia of the peripheral nervous, the schwann cells. Schwann cells originate from the neural crest and travel into the periphery to myelinate the axons of motor neurons (Woodhoo & Sommer, 2008) (Figure 6b-e).

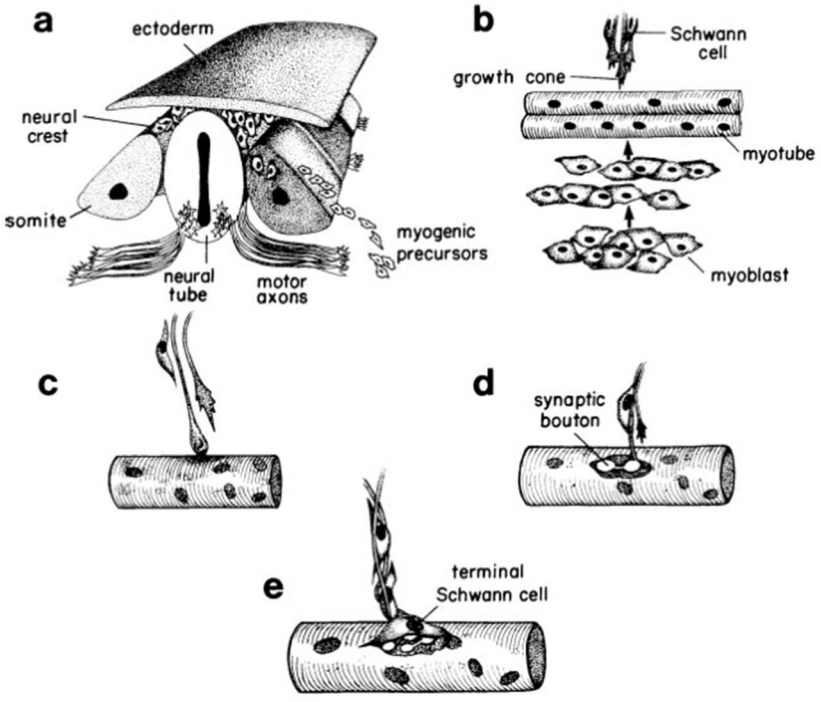

Figure 6 | Axon Formation, Axon Guidance, and Synaptogenesis

(A-E) Diagram detailing the process of axon formation, axon guidance, and synaptogenesis (Adapted from Sanes and Lichtman, 1999)

Mechanisms of Axon Guidance

Axons are the primary structure through which neurons exert their influence over targets. The process of growing an axon out into the periphery requires multiple guidance cues that ensure the axon grows in the correct direction and synapses onto the correct target. The four primary forces that act to guide the axon towards its target are chemoattraction, chemorepulsion, contact attraction, and contact repulsion (Tessier-Lavigne & Goodman, 1996) (Figure 7).

Chemorepulsive forces can be demonstrated by looking at the ephrin tyrosine kinase receptors and their ligands. As an axon makes its way into the periphery it will come across specific ephrin ligands that will bind to the growth cone and repel it. For example if an EphA receptor expressing medial motor column (MMC) motor neuron axon growth cone comes into contact with EphA ligands in the dorsal root ganglia (DRG) the axon will be prevented from entering and begin to project dorsally (Gallarda et al., 2008). Chemoattractive forces can be also be demonstrated with the MMC neurons. As mentioned before the EphA ligands prevent the axon from venturing into the DRG, but what is causing the axon to project dorsally? Fibroblast growth factors (FGFs) secreted by the dorsal epithelial cell layer, the dermomyotome, bind to the FGFR1 receptor of the MMC neurons and act as a chemoattractant for the axon (Shirasaki et al, 2006). These long-range cue signals the axon to continue traveling through the periphery, but it is important to note that there are several short-range cues that assist the axon on its journey. One example of a class of short-range cues would be the immunoglobulin cell adhesion molecules (Ig CAMS). Ig CAMS, such as NCAM, bind to the growing axon

and transduce the signaling cascade PKC that leads to actin polymerization (Li et al., 2013).

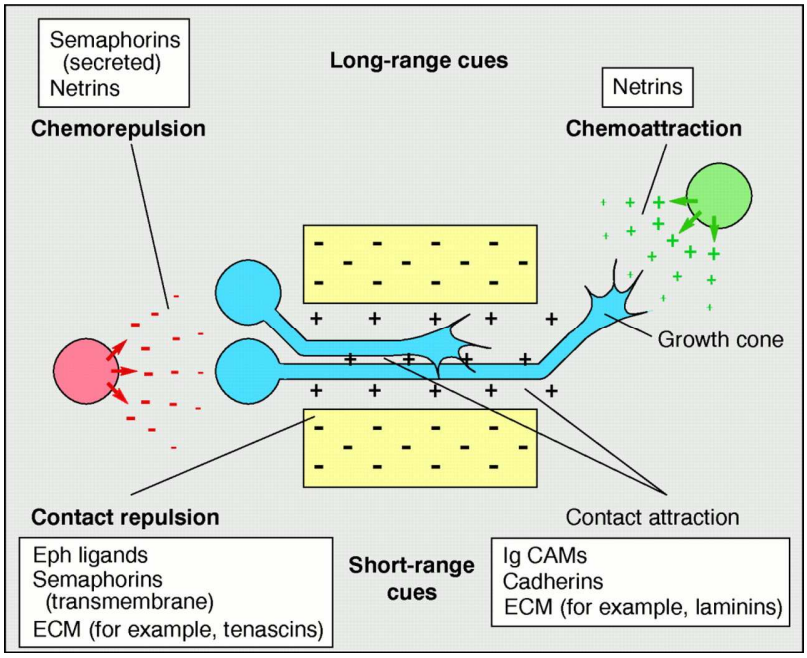

Figure 7: The Four Guidance Forces. The four forces that help guide the axon towards its proper target are chemorepulsive, contact repulsive, chemoattractive, and contact attractive (Adapted from Sanes and Lichtman, 1999)

The Neuromuscular Junction

Arguably one of the most important components of a neuron is its synapse. Throughout the nervous system there exists many different synapses that work together to create functional circuits that mediate complex behaviors. One such synapse is the neuromuscular junction (NMJ). The NMJ is the synapse formed between lower motor neurons and the skeletal muscle fibers they innervate. This synapse is crucial for the

control of muscle contraction and the execution and coordination of movement.

Acetycholine Signaling

The motor neuron signals to the muscle by releasing the neurotransmitter acetylcholine. At around E10-E11 the motor neurons complete their terminal mitosis and begin to express a detectable amount of the enzyme responsible for the synthesis of acetylcholine, choline acetyltransferase (ChAT) (Chen et al, 1992). Acetylcholine is then packaged into vesicles and sent to the synapse (Del Castillo & Katz, 1954). Here the vesicles congregate at active zones awaiting the action potential that will initiate fusion with the membrane and the release of neurotransmitter into the synaptic cleft (Sanes & Lichtman, 1999).

In order to respond to the neurotransmitter released by the motor neuron, the muscle fibers contain a high concentration of acetylcholine receptors (AChRs) numbering over 10,000/μm^2 (Salpeter & Loring, 1985). AChRs, along with voltage gated Na^+ channels, are highly concentrated into junctional folds directly apposed to presynaptic active zones, thus ensuring that neurotransmitter release at the synapse will bind to the muscle (Flucher & Daniels, 1989).

Muscle Differentiation

Initially, the density of AChRs embedded in the membrane are homogenously expressed throughout the membrane at around 1,000 per μm^2 (Bevan & Steinbach, 1977). This drastically changes as the axon begins to make contact with the newly differentiated

myotube. Once the axon establishes synaptic contact with the muscle, AChRs become circumscribed and localized underneath the site of contact, leading to a severely increased intrasynaptic/extrasynaptic ratio of AChR coverage of the muscle (Bevan & Steinbach, 1977). Numerous molecular mediators have been identified that contribute to the increase in AChR grouping underneath the overlying axon.

Agrin

Before the motor neuron synapses onto the muscle, AChRs congregate along the middle of the muscle fiber (Yang et al., 2001). Although this is an important first step, further differentiation of the NMJ requires signals from the neuron. An important secreted factor from the motor neuron in the context of NMJ formation is the proteoglycan agrin. The importance of this protein is demonstrated by the fact that mutant mice that are missing agrin fail to cluster AChRs after innervation and die before birth (Gautam et al., 1996). It is interesting to note that aneural muscle fibers are able to form AChR clusters before neuronal innervation, which indicates that neuronal agrin isn't the only source of clustering (Yang et al., 2001). This may be explained by the fact that agrin is also synthesized by muscle fibers and schwann cells, albeit it is ~1,000x less effective than neuronal agrin at AChR clustering (Gesemann et al., 1995).

MuSK

Neuronal agrin has the ability to cluster AChRs by binding to the Muscle Specific Kinase receptor (MuSK) on the muscle membrane. The activation of MuSK by Agrin

leads to MuSK's autophosphorylation, which affects many downstream signaling pathways that lead to the accumulation of proteins in the membrane of the muscle fiber (Darabid et al., 2014). In mutant mice missing MuSK receptors, AChRs fail to cluster in both aneural and neuronally innervated muscle fibers even in the presence of agrin (DeChiara et al., 1996). This suggests that MuSK plays an important role in both AChR prepatterning and in AChR clustering in response to neuronal agrin. MuSK also appears to be crucial for proper presynaptic differentiation, as MuSK mutant exhibit highly branched motor neuron terminals that cover a broader region of the muscle (Glass et al., 1996). The potency of this complex's ability to regulate synapse formation is demonstrated by the fact that ectopic expression of MuSK in agrin deficient mice rescues them from lethality (Kim & Burden, 2008).

Lrp4 and Dok7

Agrin exerts its effects of AChR clustering by binding to the MuSK co-receptor Lrp4 (Glass et al., 1996; Zhang et al., 2008). Mutant mice that lack this single-pass transmembrane protein show a similar phenotype to that of the *Musk* -/- mutant mice; AChRs fail to cluster in both aneural and neuronally innervated muscle fibers even in the presence of agrin (Weatherbee et al., 2006). The binding of agrin to Lrp4 is necessary for the clustering of AChRs by MuSK (Zhang et al., 2008). Another protein that is required for MuSK activation and further downstream activity is the adapter protein downstream-of-tyrosine-kinase-7 (Dok7). Mutant mice missing Dok7 neither form AChR clusters or NMJs (K. Okada, 2006). It is still unclear how exactly Lrp4 regulates MuSK activity, but

there are several hypotheses; by directly binding agrin or by transducing intracellular signals through an adapter protein such as Dok7 (Wu et al., 2010).

Agrin/Lrp4/MuSK Signalling Complex

How exactly MuSK activation leads to AChR clustering remained a mystery until recently. It has been shown that in response to agrin, Musk becomes rapidly internalized through receptor endocytosis by N-ethylmaleimide sensitive factor (NSF) (Zhu et al., 2008). But what exactly occurs once MuSK has been internalized? In order for AChRs to cluster themselves on the muscle membrane, there must be some sort of cytoskeletal reorganizer that allows them to properly associate with the membrane (Dai et al., 2000). It is thought that Abl1 kinase and geranylgeranyl transferase I (GGT) are some of the critical downstream mediators activated by MuSK that lead to the cytoskeletal reorganization that allows for AChR clustering (Finn et al., 2003; Luo et al., 2003). As a consequence, Rac and Rho GTPases are activated (Weston et al., 2003) One target of the activated Rho GTPase is the serine/threonine kinase Pak1. Pak1 associates to MuSK by binding to the signaling molecule Disheveled (Dvl) (Luo et al., 2002). Disruption of the interaction between MuSK and Dvl inhibits AChR clustering and inhibition of Pak1 severely reduces AChR clustering (Luo et al., 2002). Pak1 may regulate the actin dynamics of AChR clustering either by phosphorylating the cytoskeletal remodeling protein cortactin (Webb et al., 2006), by suppressing myosin light chain kinase (MLCK) and reducing the association between myosin light chains and actin (Wu 2010), or by indirectly inhibiting the activity of the actin depolymerizing factor ADF/cofilin through

the activation of LIM kinase (Lee et al., 2009).

Activity-Dependent Development of the NMJ

Acetlycholine (ACh) secreted from lower motor neurons binds to acetlycholine receptors (AChRs) on muscle fibers and causes an influx of calcium into the cytoplasm of the muscle fibers. Calcium influx activates protein kinase C (PKC), which goes on to phosphorylate the myogenic factors that participate in the transcriptional program that modulates AChR expression. It has been shown that genetic knock-out mutant mice lacking the neurotransmitter ACh have increased numbers of AChR clusters and the neuron hyper-innervates the muscle fiber (Brandon et al., 2003; An et al., PNAS 2010). Thus, neuronal activity acts as a negative regulator of lower motor neuron development that modulates neuronal morphology and differentiation of the NMJ.

Elimination

During nervous system development many neurons produce more synapses then will remain into adulthood. This plethora of synapses is often trimmed down through a process known as synaptic pruning, which is thought to contribute to proper circuit function. The mechanism that determines which synapses are eliminated and which ones survive is activity-dependent. Lower motor neurons undergo a comparable process of synaptic pruning. Instead of overtly eliminating synapses, neurons initially innervate multiple synapses (poly-neuronal

innervation) and subsequently prune projections until each NMJ is innervated by a single motor neuron (mono-neuronal innervation). During this process, as one synapse strengthens the others become weaker (Colman et al., 2017). There is also a temporal dynamic to this process, this typically occurs during the first two weeks of rodent development. It has been shown that blocking neuronal activity delays the process of synaptic pruning (Barry & Ribchester, 1995), while increasing neuronal activity accelerates the process (Duxson & Vrbová, 1985). Synaptic pruning is a competitive process. Studies show that inhibition of a single motor neuron during synaptic competition leads to a prolonged reduction in the number of innervated NMJ's compared to neighboring neurons that remain active (Buffelli et al., 2003).

Survival

During development of the nervous system approximately 50% percent of all neurons undergo programmed cell death (PCD) (Oppenheim, 1991). Many people have speculated as to why the nervous system develops such an overabundance of neurons, but one theory suggests PCD is important for control of 'systems matching' between neuronal populations and their targets (Oppenheim, 1991). The process of PCD appears to be activity-dependent as it has been shown that blocking NMJ activity leads to increased motor neuron survival (Pittman & Oppenheim, 1978). It appears that PCD in individual subsets of neurons is differentially regulated. Abolishing GABAergic and glycinergic synaptic inputs onto developing motor neurons increases limb-innervating motor neuron survival, but decreases

respiratory motor neuron survival (Banks, 2005). However, regardless of the subtype of neuron, it is obvious that activity plays an important role in the proper development of the nervous system via control of neuronal survival.

Summary

Lower motor neuron development relies upon numerous cues that activate distinct signaling pathways. These cues include the FGFs, BDNFs, WNTs, and numerous others (Stifani, 2014). It has also been shown that proper signaling both onto and from the lower motor neuron is necessary for survival (Ikonomidou, 1999). FGF signaling and activity have been shown to activate Erk/MAPK and act as crucial mediators of NMJ development (Wu et al., 2010; Tsang & Dawid, 2004; Thomas & Huganir, 2004)). Since Erk/MAPK is necessary for the proper transduction of many extracellular cues and has also been linked to activity-dependent gene regulation, we hypothesized that Erk/MAPK is necessary for lower motor neuron development. Previous research has shown that *embryonic* lower motor neuron development does not require Erk/MAPK. Here we tested whether Erk/MAPK is required for *postnatal* lower motor neuron development during important phases of activity-dependent differentiation.

Deficits in muscle development and neuromuscular control have been identified in Rasopathy patients (Johnson et al., 2011, Reinker et al., 2011, Souza et al., 2009, Stevenson et al., 2005, Tidyman et al., 2011, van der Burgt et al., 2007, & Viskochil et al., 2013). To decipher the underlying causes of muscular phenotypes found in Rasopathy patients we have also tested whether lower-motor-neuron specific changes in

Erk/MAPK are sufficient to drive abnormalities in motor behavior. An understanding of the role of Erk/MAPK in postnatal lower motor neuron development may provide insight into candidate cellular mechanisms linked to neuromuscular abnormalities found in Rasopathy patients.

CHAPTER II MATERIALS AND METHODS

Cre-Lox Recombination

The Cre-lox system is a very powerful genetic tool that allows researchers to control gene expression in specific cells at specific times. Cre-lox recombination works by inserting the gene for the Cre enzyme behind a promoter that is expressed in select cell types. This confines Cre expression, and subsequent Cre-dependent modifications, to specific cell types. Once the Cre enzyme is produced in the cell of interest it will bind engineered LoxP sites flanking the nucleic acid sequence of interest. Depending upon the orientation and placement of the loxp sites, this can work to either decrease, increase, or alter the expression of a specific gene.

Our strategy was to create a mouse model that allowed us to delete Erk/MAPK in the lower motor neurons. To do this we utilized the ChAT:Cre mouse that induces recombination at around E12 (Rossi et al., 2011). This would allow us to confine Cre expression to cholinergic expressing neurons. Past attempts to recombines Erk/MAPK in the lower motor neurons using the Olig2:Cre mouse, induced recombination at E9.5 in both lower motor neurons and oligodendrocytes and led to neonatal lethality (Newbern et al., 2011). We bred the ChAT:cre mouse model to $Erk1^{-\backslash-}$, $Erk2^{loxp/loxp}$ mice so that we could remove both Erk1 and Erk2 (Samuels et al., 2008). Erk1 can be removed from the mouse without any adverse side effects, but Erk2 cannot (Saba-el-leil et al., 2015). This is why we utilized cre-recombinase to remove Erk2. We also bred in an Ai9 reporter that produces fluorescent proteins in cells that express Cre (Madisen et al., 2010).

Transcription of the Ai9 reporter will only occur once the LoxP-flanked STOP cassette is deleted through Cre-recombination. The ChAT:Cre$^{+/-}$, Erk1$^{-\backslash-}$, Erk2$^{loxp/loxp}$, Ai9 $^{+/-}$ mouse that we generated using this strategy lives until ~P21, which allowed us to analyze early stages of postnatal lower motor neuron development.

We also generated a gain-of-function mouse model to study the effects of upregulating Erk/MAPK activity in lower motor neurons. Since most Rasopathies are due to gain-of-function mutations this mouse model would allow us to ascertain if any of the muscular phenotypes found in the Rasopathy patients were due to Erk/MAPK mutations in the motor neurons (Rauen et al., 2013). To accomplish this we bred a ChAT:Cre mouse to mouse with a constitutively active MEK1 mutation (Krenz et al., 2008). This gave us the ChAT:Cre $^{+/-}$, CaMEK$^{+/-}$ mouse. This mouse model was also bred with an Ai9 reporter.

Generation of Chat:cre, Erk1$^{-\backslash-}$Erk2$^{loxp/loxp}$, Ai9$^{+/-}$ mice

The breeding strategy outlined below is the one utilized to generate Chat:cre, Erk1$^{-\backslash-}$Erk2$^{loxp/loxp}$, Ai9$^{+/-}$ mice. Firstly, homozygous ChAT:cre (ChAT:cre$^{+/+}$) mice were bred with mice null for Erk1 and with loxp sites around Erk2 (Erk1$^{-\backslash-}$, Erk2$^{loxp/loxp}$). The progeny of this cross led to the generation of ChAT:Cre$^{+/-}$, Erk1$^{+\backslash-}$, Erk2$^{wt/loxp}$ mice. The ChAT:Cre$^{+/-}$, Erk1$^{+\backslash-}$, Erk2$^{wt/loxp}$ mice were then bred with Erk1$^{-\backslash-}$, Erk2$^{loxp/loxp}$ to generate ChAT:Cre$^{+/-}$, Erk1$^{-\backslash-}$, Erk2$^{wt/loxp}$ mice. Next, the ChAT:Cre$^{+/-}$, Erk1$^{-\backslash-}$, Erk2$^{wt/loxp}$ mouse was crossed with the an Erk1$^{-\backslash-}$, Erk2$^{oxp/loxp}$, Ai9 $^{+/+}$ mouse to generate the ChAT:Cre$^{+/-}$, Erk1$^{-\backslash-}$, Erk2$^{wt/loxp}$, Ai9 $^{+/-}$ mouse (Control) and the ChAT:Cre$^{+/-}$, Erk1$^{-\backslash-}$, Erk2$^{loxp/loxp}$, Ai9

$^{+/-}$ mouse (Mutant). These two mice served as our control and mutant for the LOF portion of our study.

Generation of ChAT:Cre $^{+/-}$, CaMEK$^{+/-}$, Ai9$^{+/-}$ mice

The breeding strategy outlined below is the one utilized to generate Chat:cre$^{+/-}$, CaMEK$^{+/-}$, Ai9$^{+/-}$ mice. Firstly, homozygous CaMEK (CaMEK$^{+/+}$) were bred with Ai9$^{+/+}$ mice. The progeny of this cross led to CaMEK$^{+/-}$, Ai9$^{+/-}$ mice. The CaMEK$^{+/-}$, Ai9$^{+/-}$ mice were breed with CaMEK, Ai9$^{+/+}$ mice to generate CaMEK$^{+/+}$, Ai9$^{+/+}$ mice. The CaMEK$^{+/+}$, Ai9$^{+/+}$ mice were then breed with ChAT:Cre$^{+/+}$ mice. This generated ChAT:Cre$^{+/-}$ CaMEK$^{+/-}$, Ai9$^{+/-}$ mice (mutant) and ChAT:Cre$^{+/-}$, Ai9$^{+/-}$ mice (control). These two mice served as our control and mutant for the GOF portion of our study.

Genotyping

Toe samples were taken using sharp scissors from juvenile pups (~P6-P10) to serve as tissue for genotyping material. The toes were individually placed into eppendorf tubes, lysis buffer was added to extract the DNA from the tissue, and the solution was heated to 50C for 30 minutes. Once the DNA was extracted, neutralizing buffer was added to the solution. The DNA samples were added to a mixture of Taq Polymerase, clean H_20, and primers for actin, Erk2 loxP sites, CaMEK, and Ai9. The PCR program was set to denature the DNA at 95°C for 20 seconds, anneal primers at 60°C for 30 seconds, and extend at 72°C for 30 seconds. This cycle was repeated 32 times. The sample was then cooled to 4°C. Once PCR amplification of the DNA was completed it

was placed into the electrophoresis gel. The gel was created by mixing 100ml TBE with 1.8g agarose, heating it in the microwave for 90 seconds, pouring the mixture into a mold with EtBr, and allowing it to cool. Once the gel had solidified the amplified DNA was placed into individual wells and let run in the electrophoresis machine at 145V for 30min. The genotyping was then scanned and read to determine the genotype of our mice.

Tissue Collection

Perfusion and Tissue Collection

Mice were anesthetized through IP injection of 200-400mg/kg tribromoethanol (Avertin). Once the mice were completely unconscious each mouse was pinned to a dissection tray. An incision was made below the sternum and, once exposed, the diaphragm was cut away. The rib cage was lifted and two parallel cuts were made thus exposing the heart. Using hemostats, the ribcage was lifted away to fully expose the heart. To perfuse the heart a peristaltic pump was used. The perfusion needle was inserted into the left ventricle of the heart and a small incision was made in the right atrium. The pump was activated and set to perfuse 5-10mL of 1X PBS into the circulatory system of the mouse. Once 1-2 minutes passed or once the liquid expelling from the right became clear, 15-30mL of 4% PFA/PBS was perfused into the mouse. The following samples were removed from the mice: Brain, cervical enlargement of the spinal cord, lumbar enlargement of the spinal cord, soleus, gastrocnemius, and diaphragm.

Cryopreservation

The next step was to freeze down the samples in OCT (Optimal cutting temperature compound) for either long-term storage or cryostat usage. To ensure that the samples didn't form ice crystals while being frozen, the samples were immersed in a sucrose solution. The sucrose solution penetrates the tissue and acts as a cryoprotectant. To begin the mouse brain was placed into a solution of 15% sucrose over the first night and then placed in a solution of 30% sucrose over the second night. A similar protocol was used for the muscles and spinal cord segments, except the first night is skipped and samples are only immersed in 30% sucrose for one night.

Once the samples were properly saturated with sucrose the freezing could begin. In a rubber ice bucket bath of 70% ethanol and dry ice was made. While this was cooling small square molds (2x2x2in) were made using aluminum foil. The molds were filled with OCT and each of the samples was individually suspended in the OCT molds. The OCT molds were slowly lowered into the ethanol/dry ice bath and allowed to sit until completely frozen. Once frozen the samples were placed into long-term storage or immediately sectioned using the cryostat.

Cryosectioning

The OCT blocks containing the samples were placed into a cryostat for 30 minutes to allow the blocks to equilibrate to the temperature. The temperature varied depending on the tissue type; muscle was sectioned at -16 °C and the spinal cord segments were sectioned at -18 °C. Once the OCT block had time to equilibrate to the temperature of the cryostat it was placed secured to a sample stud using OCT and

attached to the chuck. The cryostat section thickness was then adjusted to 40μm for spinal cord segments and 80μm for muscles. As each section came off the plate it was placed onto a Superfrost Plus microscope slide with a fine-bristled brush.

Immunohistochemistry

The Superfrost Plus microscope slides containing the samples were attached to the slides by incubation on a slide warmer at 50°C for 10 minutes. The slides were then removed and circled with a PAP pen to create a reagent confinement zone. The slides were rinsed twice in a solution of PBS/0.05% Triton X-100 (PBST) for 10 minutes. The slides were then rinsed with PBS. The slides were then placed into a humidified slide chamber with 1ml of blocking solution (5%NDS/PBST) added to the slides and allowed to incubate for 30 minutes at room temperature. Once completed, the blocking solution was poured off the slides and primary antibodies diluted in blocking solution were added to the slides. The following primary antibodies were used: Sigma Aldrich DAPI (1:1000), Life Technologies a-Bungarotoxin Alexa Fluor 488 Conjugate (1:1000), Rockland Anti-RFP Chicken Antibody (1:1000), Rockland Anti-RFP Rabbit Antibody (1:1000), SV2 (1:1000), BioLegend Purified anit-Tubulin B3 (TUBB3, Clone: TUJ1)(1:1000), Millpore NeuN (1:1000), Millpore Anti-Choline Acetyltransferase (1:1000), Abcam Rb mAb to Erk2 [E460] (1:1000), and Abcam Rb Ab to Mek1 [E342]. The slides were placed into a humidified slide chamber and allowed to incubate overnight at 4°C. After the overnight incubation, the slides were rinsed three times in a solution of PBST for 60 minutes. The slides were then placed back into the humidified slide chamber with secondary antibodies

diluted in blocking solution added to the slides. The following secondary antibodies were used: Alexa Fluor 488 Donkey anti-mouse (1:1000), Alexa Fluor 488 Donkey anti-rabbit (1:1000), Alexa Fluor 488 Donkey anti-goat (1:1000), Alexa Fluor 555 Donkey anti-mouse (1:1000), Alexa Fluor 555 Donkey anti-mouse (1:1000), Alexa Fluor 567 Donkey anti-mouse (1:1000), and Alexa Fluor 647 Donkey anti-mouse (1:1000). The slides were allowed to incubate overnight at 4°C. After the overnight incubation, the slides were rinsed three times in a solution of PBS for 30 minutes. Once completed, excess buffer was removed and slides were coverslipped with Fluoromount.

Histochemical Analysis

Motor Neuron Counts

To assess motor neuron survival, sections from the L4-L5 region of the spinal cord were sampled. Ai9 positive lower motor neurons from the lateral motor column were counted from every fourth 40μm section throughout the entire L4-L5 region of the spinal cord. The observer was blinded to experimental group. The average number of motor neurons were calculated for the entire region and compared between mutant and control.

Plaque-to-Pretzel

To assess whether the NMJs of the mice had properly transitioned from a plaque shaped morphology to a pretzel shaped morphology we performed a qualitative assessment. The observer was blinded to experimental group. Ten BTX-labeled NMJs

from every 3rd 80μm section of the gastrocnemius muscle were randomly chosen for morphology assessment until ~100 were measured. The morphologies of the NMJs were characterized as either being plaque, transitioning, or pretzel. The percentage of plaque shaped, transitioning, and pretzel shaped NMJs of three pairs of control/mutant mice were then compared.

NMJ Area

To assess for the total area of the average NMJ we performed a quantitative measurement. 5 BTX-labeled NMJs from every 3rd 80μm section of the gastrocnemius muscle were randomly chosen until 50 were measured. The observer was blinded to experimental group. Area measurements were taken from three control/mutant pairs of mice using the LASX Leica software.

Poly-to-Mono Counts

To assess the if NMJs had undergone the process of synaptic pruning we analyzed 150 random Ai9 expressing NMJs from the gastrocnemius muscle and determined if they were poly-neuronally innervated or mono-neuronally innervated. The observer was blinded to experimental group. The number of poly-neuronal vs. mono-neuronal NMJs were then compared across three age-matched pairs.

Behavioral Testing

Rotarod

Rotarod was used to assay the ability of the mice to coordinate their limbs and ascertain if any motor defects were present. The rotating platform was programmed to increase from 0 to 40 RPMs over the period of 5 minutes. This was repeated for 3 trials a day with 15 minutes in between each trial. This was repeated for 5 days.

Open Field

To perform the open field assay we acquired a 40cm x 40cm x 40cm plastic box and positioned a camera and light above it. The light was positioned to illuminate the box while the camera acquired video. The behavioral assay consisted of placing the mouse into the box while it's pattern of activity was recorded for 10 minutes. We analyzed the video with the Open Field plug-in for ImageJ.

Rope Test

A vertical rope-climbing test was used to assay both motor coordination and grip strength. The assay involved placing a mouse at the bottom of a suspended nylon rope (50cm length, 1-1.5cm thickness) with regularly placed knots. The rope was suspended 45cm above a large box filled with padding (foam blocks) to protect the mice from injury if they should fall. The box of foam was covered with thin plastic sheeting so that any waste dropping from the climbing mouse didn't contaminate the foam. The time it takes the mouse to ascend the rope was measured. Trials were stopped after 2 minutes. This was done on one day with three trials per mouse.

Weighted Object Test

For this assay, the ability of the mouse to lift a metal weight was tested. A metal scouring pad was attached to a metal weight (steel chain links ranging from 5-85g) and placed in front of the mouse. Once the mouse grabbed the scouring pad, it was slowly raised by the base of its' tail until the entire weight was suspended in the air. If the mouse dropped the weight, the trial was repeated until three attempts were made. If the mouse was able to hold the weight in the air for 3 seconds, it was gently placed back onto the table and tested at the next increment in weight. This was repeated until the mouse was unable to hold the weight in the air for three seconds in at least one of three attempts. The test included one day of habituation and one testing day.

Morris Water Maze

To test the memory and swimming ability of the mice we utilized the Morris Water Maze. A metal pool was filled with water until the hidden platform lay just below the surface of the water. To ensure that the mouse wouldn't be able to see the platform, non-toxic white paint was added to the water until the platform wasn't visible. Symbols were added to the walls of the room to provide spatial cues for the mouse to remember the location of the platform. To perform the assay, mice were placed into a random quadrant of the pooled and allowed to swim for 60 seconds. If the mouse finds the platform it is left to rest for 15 seconds before being dried off and placed onto a heating pad. If the mouse couldn't find the platform in 60 seconds it was led to the platform and left to rest for 15 seconds before being dried off and placed onto a heating pad. This was repeated for 4 trials per day with 15 minutes of rest in between each trial over a period of

5 days. On the 5th day mice underwent a 5th trial consisting of a probe test. This involved taking the platform away from the pool to observe the swimming strategy employed by the mouse. Video was then scored using the Water Maze ImageJ plugin.

CHAPTER III - LOSS OF FUNCTION ERK/MAPK RESULTS

To assess the requirement of Erk/MAPK signaling in postnatal lower motor neuron development we developed a mouse model where Erk1/2 was deleted in lower motor neurons in a Chat:cre, $Erk1^{-\backslash-}Erk2^{loxp/loxp}$ model. This model allowed us to successfully confine Erk/MAPK deletion to cholinergic expressing neurons. Even though the mutant mice died by three weeks of age, we were able to assess the postnatal development of lower motor neurons in the absence of Erk/MAPK during critical stages of early postnatal development. Previous attempts to assess Erk/MAPK function in the spinal cord used a similar strategy with an Olig2:Cre mouse (Newbern et al., 2011). This mouse model induced recombination at E9.5 in the spinal cord progenitor domain that produces motor neurons and oligondendrocytes, however, mutants died at birth. Thus, the Chat:cre, $Erk1^{-\backslash-}Erk2^{loxp/loxp}$, $Ai9^{+/-}$ mouse provides a unique opportunity to cell-autonomously assess the postnatal development of lower motor neurons in the absence of Erk/MAPK.

Mouse Model Confirmation: Choline Acetyltransferase Expression

To assess whether we successfully induced the mutation in the lower motor neurons of the Chat:cre, $Erk1^{-\backslash-}Erk2^{loxp/loxp}$, $Ai9^{+/-}$ mice, we performed immunohistochemical analysis of L4 lumbar spinal cord segments. We performed this analysis for three mutants and three controls. We found that all Ai9 expressing cells colocalized with ChAT expression, which confirmed that our reporter was in the lower motor neurons (Figure 8).

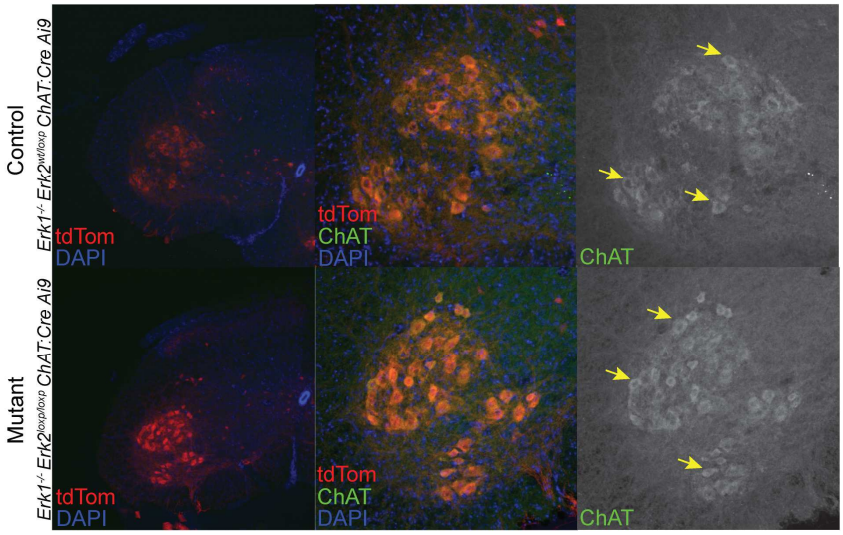

Figure 8: LOF P18 ChAT Expression

Mouse Model Confirmation: Erk2 Expression

To assess whether our mutation worked in the Chat:cre, $Erk1^{-/-}Erk2^{loxp/loxp}$, $Ai9^{+/-}$ mice we performed an immunohistochemical analysis of Erk2. We performed this analysis for three mutants and three controls. The mutants exhibited a complete loss of Erk2 expression in Ai9-expressing lower motor neurons relative to controls (Figure 9).

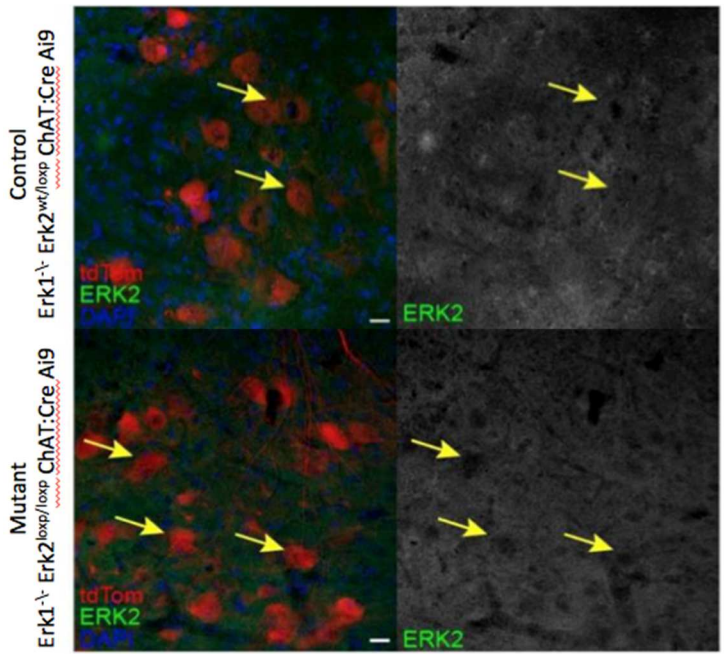

Figure 9: P18 LOF ERK2 Expression

Motor Neuron Counts

In order to assay motor neuron survival in the Chat:cre, $Erk1^{-\backslash-}Erk2^{loxp/loxp}$, $Ai9^{+/-}$ mice we counted the average number of Ai9 expressing motor neurons from every fourth 40µm slice of the L4-L5 region of the lateral motor column within the spinal cord of the mice and compared the number to age matched P18 controls (Figure 10). We performed this analysis for three mutants and three controls. We found an average number of 36.69±8.95 motor neurons per section in the mutant compared to an average number of 38.56±9.97 of motor neurons per section in the control (Figure 11). The result of a two-tailed t-test revealed a non-significant value of 0.41. Thus, Erk/MAPK does not appear to be necessary for lower motor neuron survival.

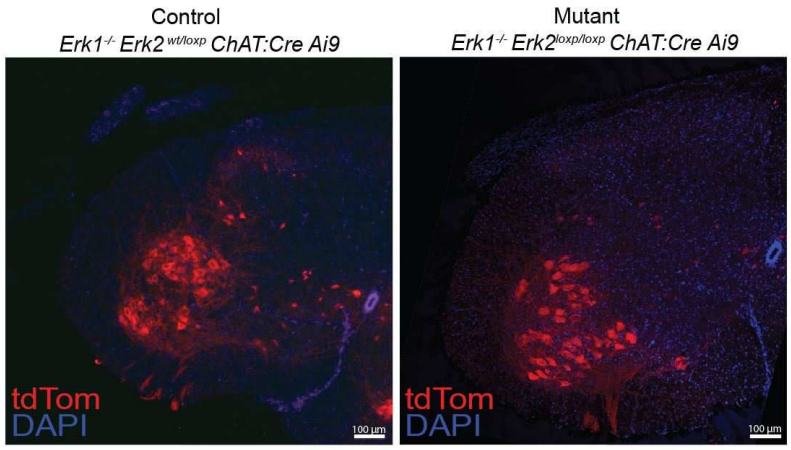

Figure 10: LOF P18 L4 Region of the Spinal Cord

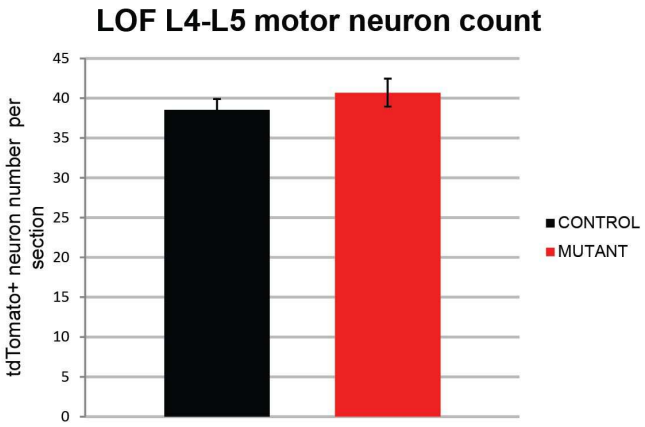

Figure 11: LOF P18 Motor Neuron Counts

NMJ Area

In order to assay the total area that AChRs took up in the NMJs of the Chat:cre, $Erk1^{-\backslash-}Erk2^{loxp/loxp}$, $Ai9^{+/-}$ we measured the area of 50 BTX labeled NMJs and compared the results to age matched P18 controls. We performed this analysis for four mutants and four controls. We found that the average area of NMJs in the mutant was

266.84μm^2±16.56μm^2 compared to the average area of 258.47μm^2±11μm^2 in the control (Figure 12). The result of a two-tailed t-test revealed a non-significant value of 0.43.

The analysis was also done for Chat:cre, Erk1$^{-\backslash-}$Erk2$^{loxp/loxp}$, Ai9$^{+/-}$ mice at P10 and their age match controls. We performed this analysis for three mutants and three controls. We found that the average area of NMJs in the mutant was 139.13μm^2±13.52μm^2 compared to the average area of 167.04μm^2±26.41μm^2 in the control (Figure 12). The result of a two-tailed t-test revealed a non-significant value of 0.18. The results of this assay provided strong evidence that the area of the postsynaptic portion of the NMJ is independent of Erk/MAPK.

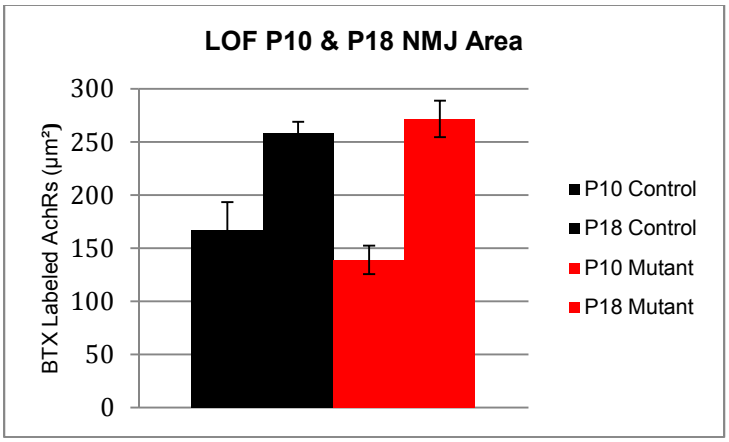

Figure 12: LOF P10 & P18 NMJ Area

Presynaptic NMJ Area

In order to analyze the total area that the axon took up on the NMJs of the Chat:cre, Erk1$^{-\backslash-}$Erk2$^{loxp/loxp}$, Ai9$^{+/-}$ we measured the area of 20 Ai9 expressing NMJ synapses and compared the results to age matched P10 controls. We performed this analysis for three mutants and three controls. We found that the average area of Ai9

expressing NMJ synapses in the mutant was 58.04μm^2±19.31μm^2 compared to the average area of 73.28μm^2±5.32μm^2 in the control (Figure 13). The result of a two-tailed t-test revealed a non-significant value of 0.26. The results of this assay provided strong evidence that the area of the presynaptic portion of the NMJ is independent of Erk/MAPK.

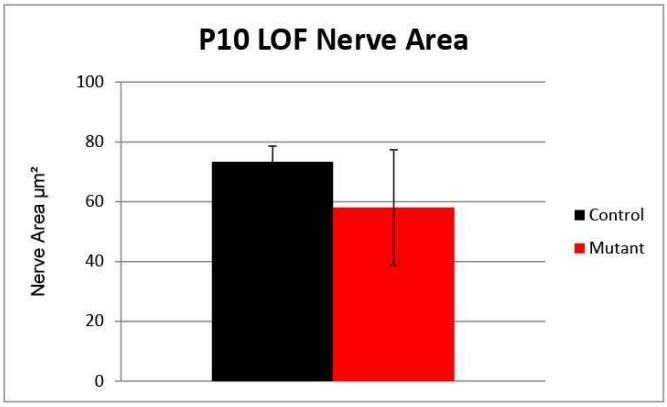

Figure 13: LOF P10 Area of the Presynaptic Portion of the NMJ

Presynaptic NMJ Binary Masking

We performed a qualitative analysis of the presynaptic membrane of the Chat:cre, Erk1$^{-\backslash-}$Erk2$^{loxp/loxp}$, Ai9$^{+/-}$ mice by converting images of the NMJs into monochrome images. These images were compared to those of a P10 age matched control. We performed this analysis for three mutants and three controls. We found no noticeable difference between the appearance between the mutants and controls (Figure 14). In summary, we conclude that ERK/MAPK signaling is not necessary for the development of the size of pre- or post-synaptic structure during NMJ differentiation.

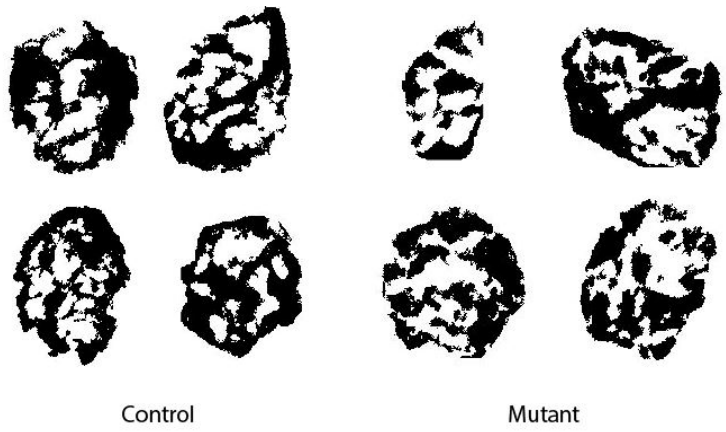

Figure 14: Structural Analysis of the Presynaptic Portion of the LOF NMJ

Plaque to Pretzel

To determine if the NMJs of the Chat:cre, $Erk1^{-\backslash-}Erk2^{loxp/loxp}$, $Ai9^{+/-}$ mice had properly matured we assessed the morphology of 315 random BTX labeled NMJs from the gastrocnemius muscle across three mutants and 310 random BTX labeled NMJs across three age-matched P18 controls (Figure 15). We found an average of 40±10.44 of the NMJs in the mutant were still in the plaque phase of maturation compared to 18.67±3.51 in the control, 62.67±11.85 were transitioning in the mutant compared to 50.33±10.69 in the control, and only 2.33±2.52 matured into a pretzel-shaped morphology in the mutant compared to 37.67±12.02 in the control (Figure 16). The results of two-tail t-tests for the three analyses revealed a significant difference between the percentage of NMJs still in the plaque phase ($p=0.03$) and the percentage of NMJs that had matured to the pretzel phase ($p=0.01$). The t-test for the percentage of NMJs that were transitioning yielded non-significance ($p=0.25$). The results of this assay indicate that the proper morphological change from plaque-to-pretzel at the NMJ is Erk/MAPK

dependent.

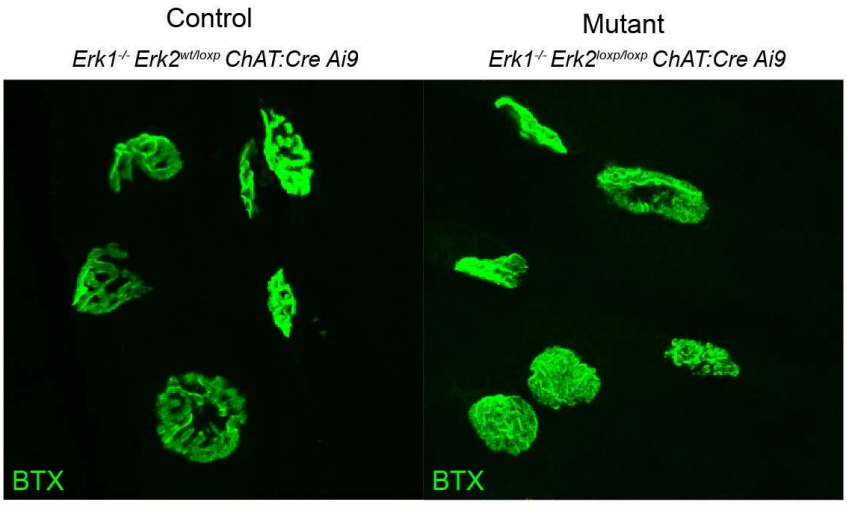

Figure 15: LOF P18 Plaque to Pretzel Qualitative Analysis

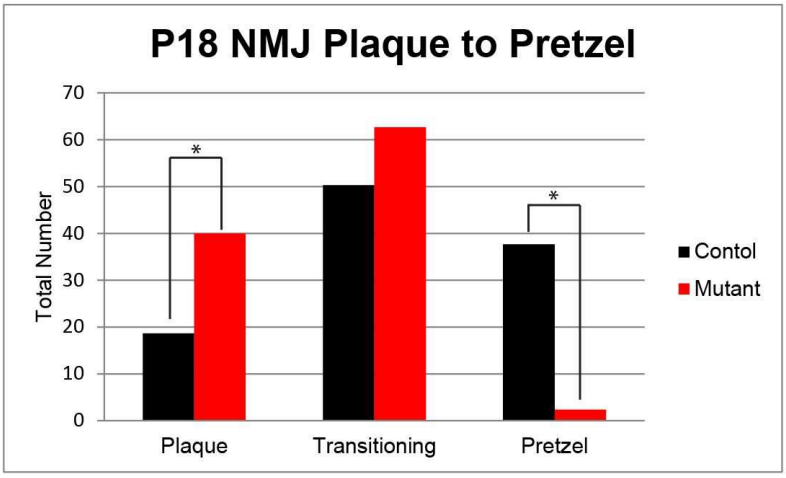

Figure 16: LOF P18 NMJ Plaque to Pretzel Quantitative Analysis

The analysis was also done for Chat:cre, $Erk1^{-\backslash-}Erk2^{loxp/loxp}$, $Ai9^{+/-}$ mice at P10 and their age match controls. We performed this analysis for three mutants and three controls. We found that 71.08%±1.77 of the NMJs in the mutant were still in the plaque

phase of maturation compared to 57.25%±5.86% in the control and 28.92%±1.77% were transitioning in the mutant compared to 42.75%±5.86% in the control (Figure 17). The results of two-tail t-tests revealed a significant difference between the percentage of NMJs still in the plaque phase (p=0.02) and the percentage of NMJs that had entered the transitional phase (p=0.02). The results of this assay indicate that even at earlier stage of postnatal development that the proper morphological change from plaque-to-pretzel at the NMJ is Erk/MAPK dependent.

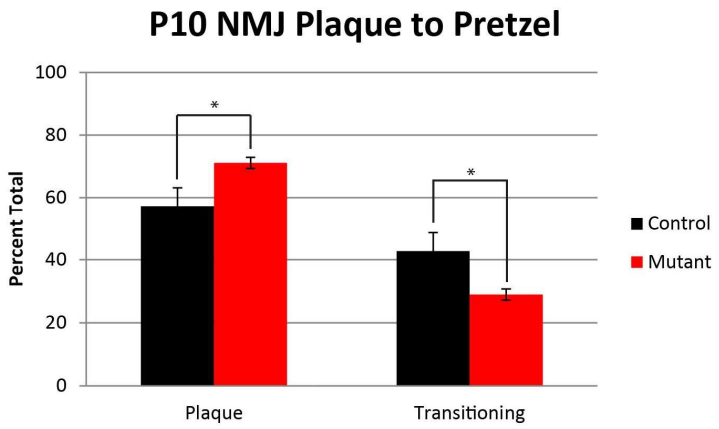

Figure 17: LOF P10 NMJ Plaque to Pretzel Quantitative Analysis

Poly-to-Mono Counts

To assess whether the NMJs of the Chat:cre, $Erk1^{-\backslash-}Erk2^{loxp/loxp}$, $Ai9^{+/-}$ underwent the process of poly-neuronal innervation to mono-neuronal innervation we counted the number of synapsing axon found at 150 random Ai9 expressing NMJs from the gastrocnemius muscle and compared them to age matched P18 controls. We performed this analysis for three mutants and three controls. The average number of NMJs in the

mutant that were poly-neuronally innervated was 4.39%±4.39% compared to 3.26%±2.82% in the control (Figure 18, 20). The average number of NMJs in the mutant that were mono-neuronally innervated was 95.61%±3.41% compared to 96.74%±2.82% in the control (Figure 19, 20). The result of two-tailed t-tests for both of the analyses revealed non-significant values of 0.68. It can be concluded that the transition from poly-to-mono neuronal innervation is Erk/MAPK independent.

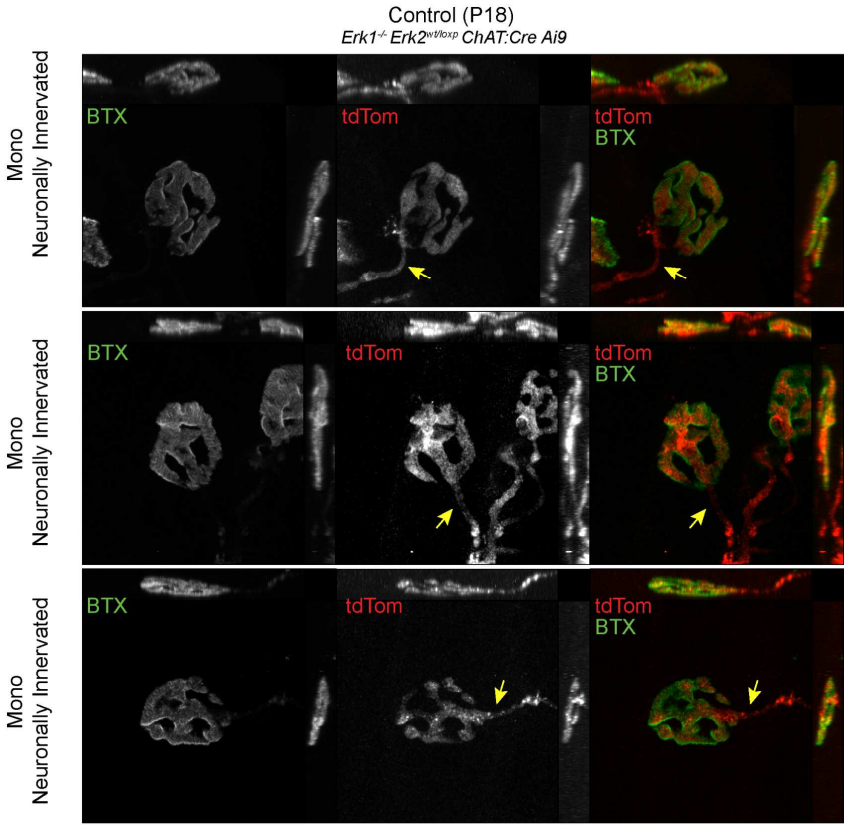

Figure 18: LOF P18 Control Poly-to-Mono Qualitative Analysis

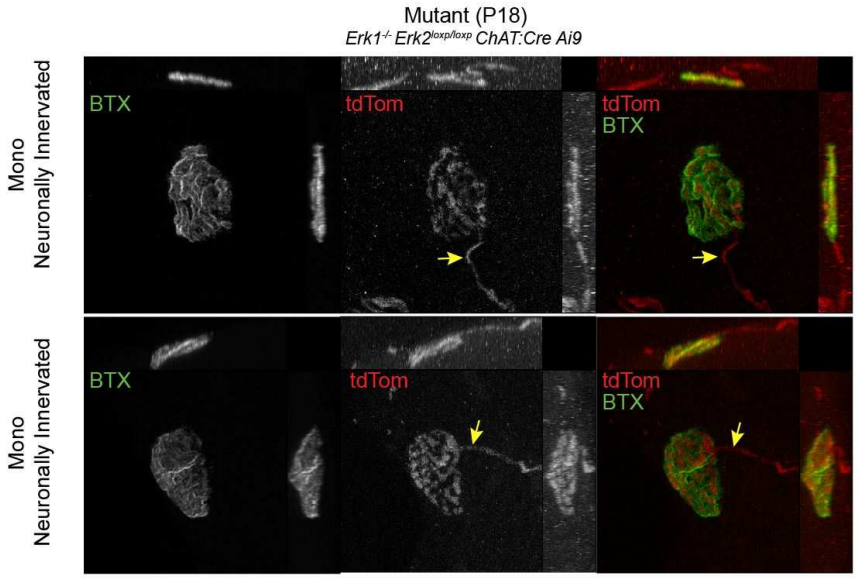

Figure 19: LOF P18 Mutant Poly-to-Mono Qualitative Analysis

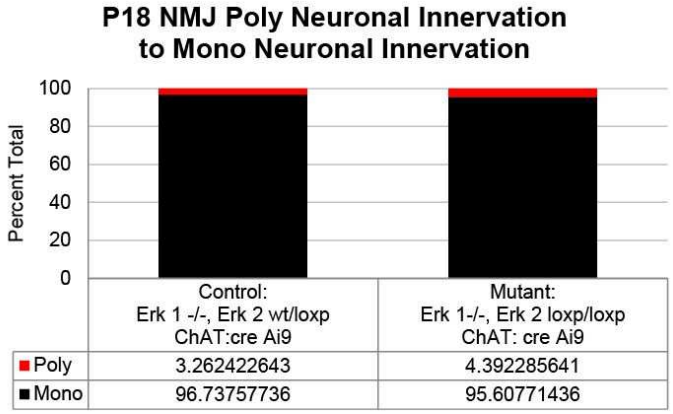

Figure 20: LOF P18 Poly-to-Mono Quantitative Analysis

In order to ascertain the rate at which NMJs of the Chat:cre, $Erk1^{-\backslash-}Erk2^{loxp/loxp}$, $Ai9^{+/-}$ mice undergo synaptic pruning we counted the number of synapsing axons found at 150 random Ai9 expressing NMJs from the gastrocnemius muscle and compared them to age matched P10 controls. We performed this analysis for three mutants and three

controls. The average number of NMJs in the mutant that were poly-neuronally innervated was 13.17%±7.86% compared to 7.04%±3.7% in the control (Figure 21). The average number of NMJs in the mutant that were mono-neuronally innervated was 86.83%±7.86% compared to 92.96%±3.7% in the control. The result of two-tailed t-tests for both of the analyses revealed non-significant values of 0.29. The results of this assay indicate that the rate at which the NMJs experience synaptic pruning is similar between the mutants and controls.

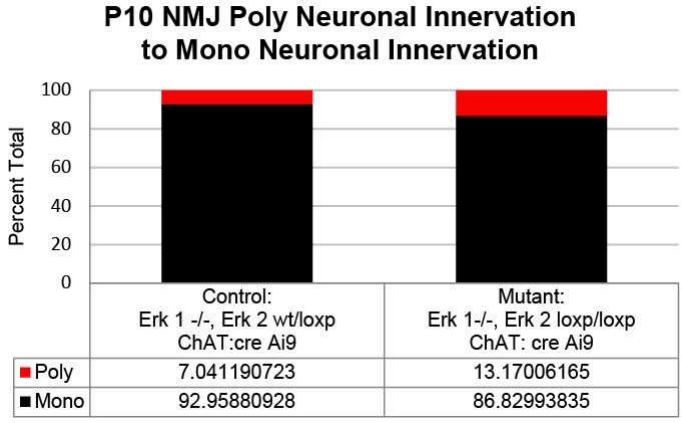

Figure 21: LOF P10 Poly-to-Mono Quantitative Analysis

Synaptic Vesicle Clustering

To uncover whether the NMJs of Chat:cre, $Erk1^{-/-}Erk2^{loxp/loxp}$, $Ai9^{+/-}$ mice exhibited normal clustering of vesicles in the presynaptic portion of the NMJ we performed immunohistochemical analysis with the SV2 antibody. We performed this analysis for three mutants and three controls. We found that both mutants and controls exhibited normal clustering of vesicles confined to the most distal part of the synapses (Figure 22).

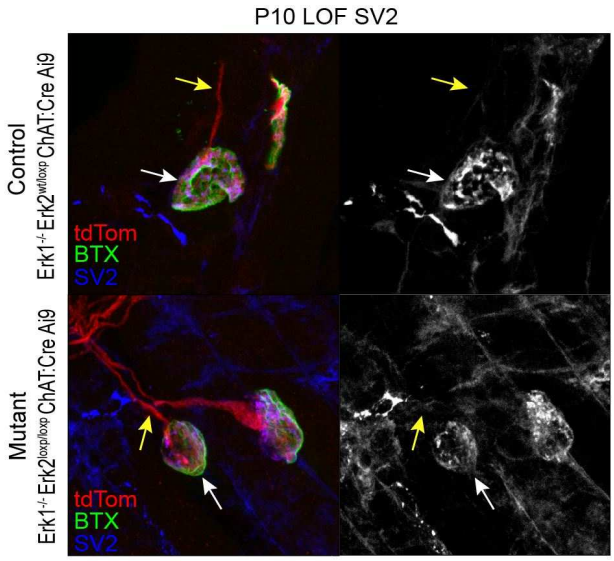

Figure 22: LOF P18 Synaptic Clustering

Mouse Model Confirmation: Choline Acetyltransferase Expression

To assess whether we successfully induced the mutation in the lower motor neurons of the ChAT:Cre $^{+/-}$, CaMEK$^{+/-}$, Ai9$^{+/-}$ mice, we performed immunohistochemical analysis of L4 lumbar spinal cord segments. We performed this analysis for three mutants and three controls. We found that all Ai9 expressing cells colocalized with ChAT expression, which confirmed that our reporter was in the lower motor neurons (Figure 23).

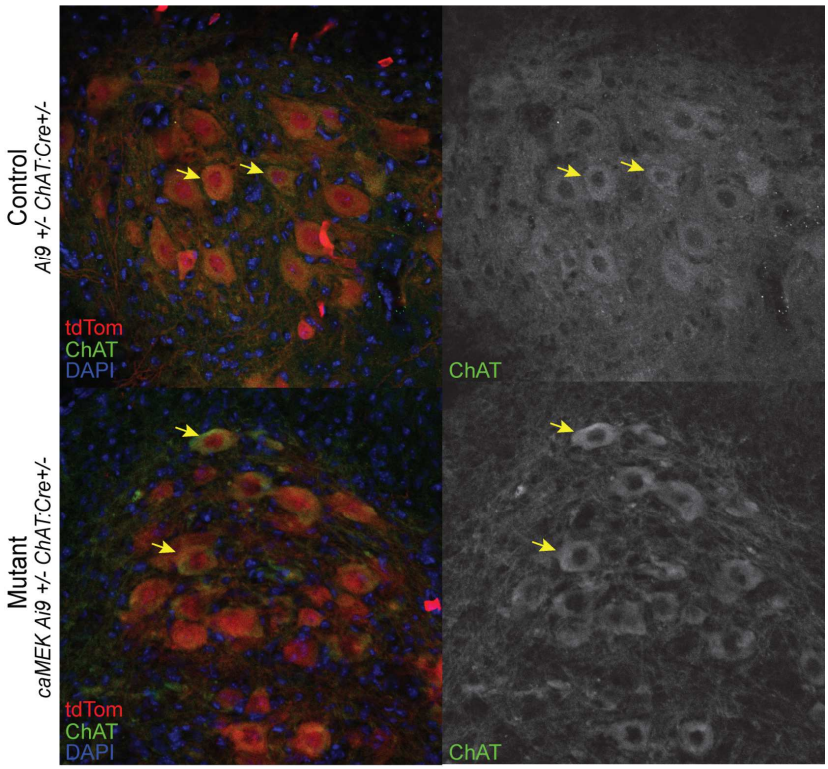

Figure 23: GOF P60 ChAT Expression

Mouse Model Confirmation: MEK Expression

To assess whether the mutation worked in the ChAT:Cre $^{+/-}$, CaMEK$^{+/-}$, Ai9$^{+/-}$ mouse model we performed an immunohistochemical analysis of MEK1. We performed this analysis for three mutants and three controls. The mutants exhibited higher MEK1 expression in lower motor neurons than the controls (Figure 24).

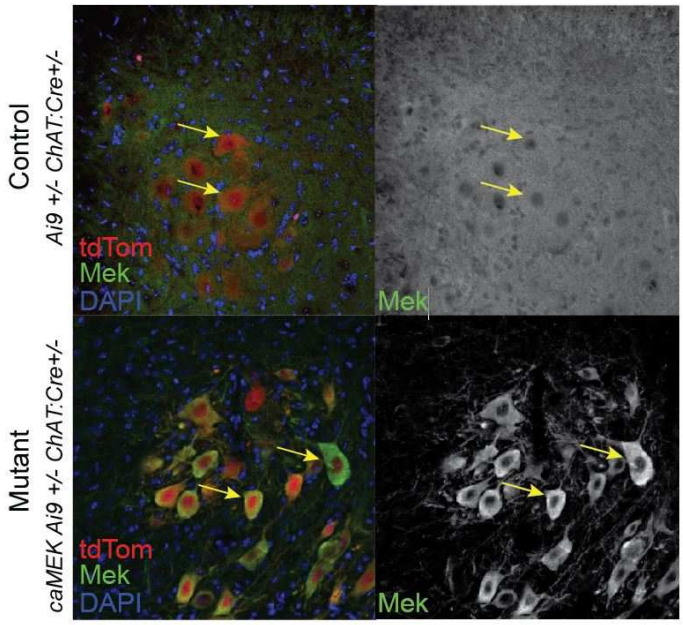

Figure 24: GOF P60 MEK Expression

Motor Neuron Counts

To assess motor neuron survival in the ChAT:Cre $^{+/-}$, CaMEK$^{+/-}$, Ai9$^{+/-}$ mice we counted the average number of Ai9 expressing motor neurons from every fourth 40µm slice of the L4-L5 region of the lateral motor column within the spinal cord of the mice and compared the number to age matched P10 controls (Figure 25). We performed this

analysis for three mutants and three controls. We found an average number of 34.52±1.37 in the mutant compared to an average number of 34.81±3.64 in the control (Figure 26). The result of a two-tailed t-test revealed a non-significant value of 0.87. Thus we can conclude that upregulation of Erk/MAPK has no noticeable effect on motor neuron count.

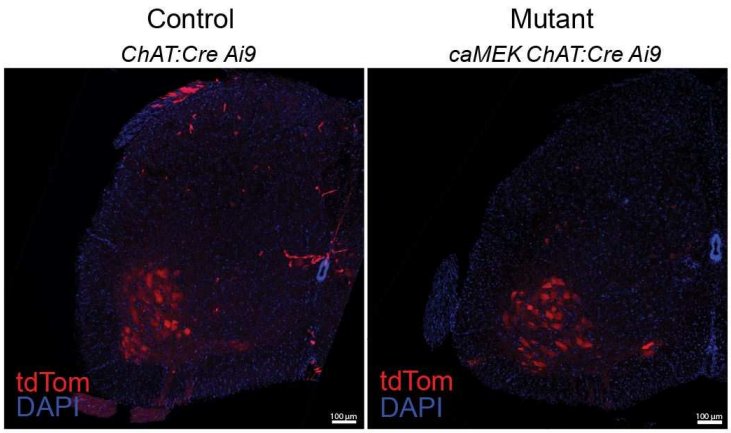

Figure 25: GOF P60 L4 Region of the Spinal Cord

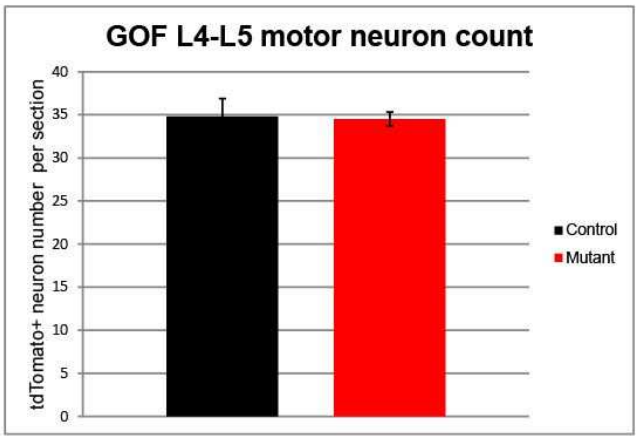

Figure 26: GOF P60 Motor Neuron Counts

NMJ Area

To assess the total area that AChRs took up in the NMJs of the Chat:cre, CaMEK$^{+/-}$, Ai9$^{+/-}$ we measured the area of 50 BTX labeled NMJs and compared the results to age matched P60 controls. We performed this analysis for three mutants and three controls. We found that the average area of NMJs in the mutant was 420.48μm^2±28.78μm^2 compared to the average area of 414.25μm^2±2.8μm^2 in the control (Figure 27). The result of a two-tailed t-test revealed a non-significant value of 0.73. The results of this assay indicate that the upregulation of Erk/MAPK has no noticeable effect on NMJ area at P60.

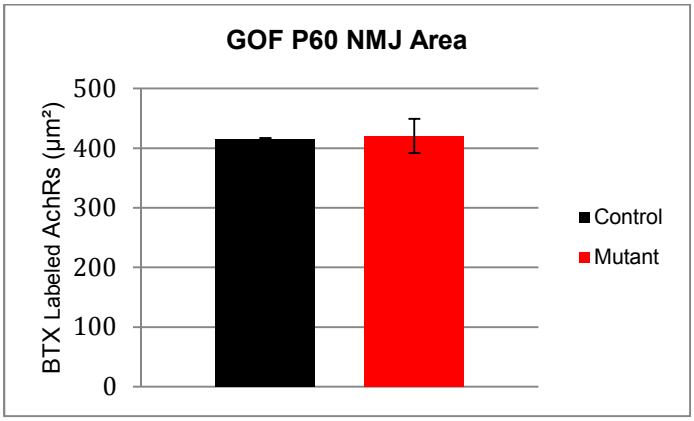

Figure 27: GOF P60 Quantitative Analysis of NMJ Area

The analysis was also done for Chat:cre, CaMEK$^{+/-}$, Ai9$^{+/-}$ mice at P10 and their age match controls. We performed this analysis for three mutants and three controls. We found that the average area of NMJs in the mutant was 171.59μm^2±22.52μm^2 compared to the average area of 162.22μm^2±20.85μm^2 in the control (Figure 28). The result of a two-tailed t-test revealed a non-significant value of 0.62. The results of this assay indicate that the upregulation of Erk/MAPK has no noticeable effect on NMJ area at P10.

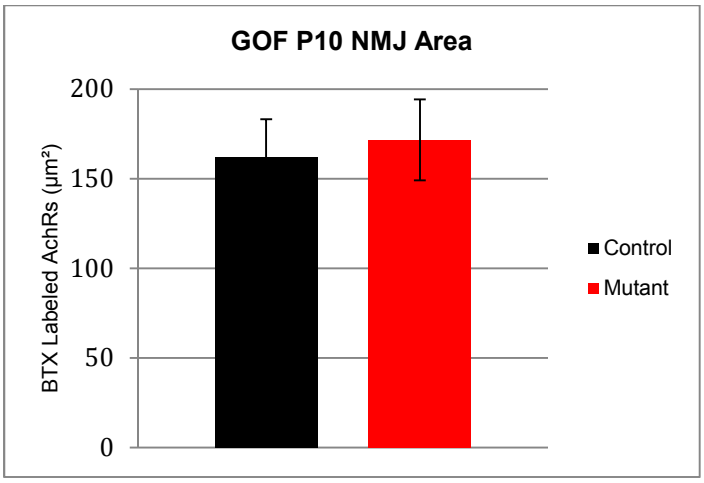

Figure 28: GOF P10 Quantitative Analysis of NMJ Area

Plaque-to-Pretzel

To determine if the NMJs of the Chat:cre, CaMEK$^{+/-}$, Ai9$^{+/-}$ mice were properly maturing we assessed the morphology of 100 random BTX labeled NMJs from the gastrocnemius muscle and compared them to age matched P10 controls. We performed this analysis for three mutants and three controls. We found that 65.12%±12.8% of the NMJs in the mutant were still in the plaque phase of maturation compared to 60.96%±9.06 in the control and 34.88%±12.18% were transitioning in the mutant compared to 39.04% ±9.06% in the control (Figure 29). The results of two-tail t-tests yielded a non-significant difference between the percentage of NMJs still in the plaque phase ($p=0.66$) and the percentage of NMJs that had entered the transitional phase ($p=0.66$). Thus we can conclude that an upregulation of Erk/MAPK doesn't affect the proper morphological maturation of the NMJ from plaque-to-pretzel.

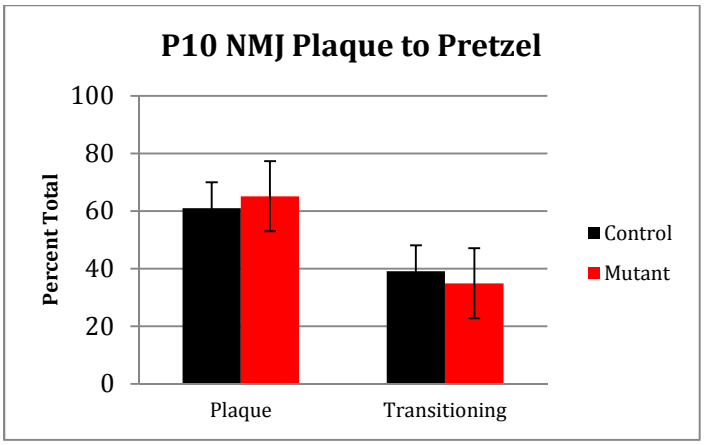

Figure 29: GOF P10 Plaque to Pretzel Quantitative Analysis

Poly-to-Mono Counts

To assess the rate at which NMJs of the Chat:cre, CaMEK$^{+/-}$, Ai9$^{+/-}$ mice undergo synaptic pruning we counted the number of synapsing axon found at 150 random Ai9 expressing NMJs from the gastrocnemius muscle and compared them to age matched P10 controls. We performed this analysis for three mutants and three controls. The average number of NMJs in the mutant that were poly-neuronally innervated was 11.78%±8.77% compared to 8.9%±6.7% in the control (Figure 30). The average number of NMJs in the mutant that were mono-neuronally innervated was 88.22%±8.77% compared to 91.1%±6.7% in the control. The result of two-tailed t-tests for both of the analyses revealed non-significant values of 0.29. Thus we can conclude that the temporal dynamics of synaptic pruning are left intact in the presence of an upregulation of Erk/MAPK activity.

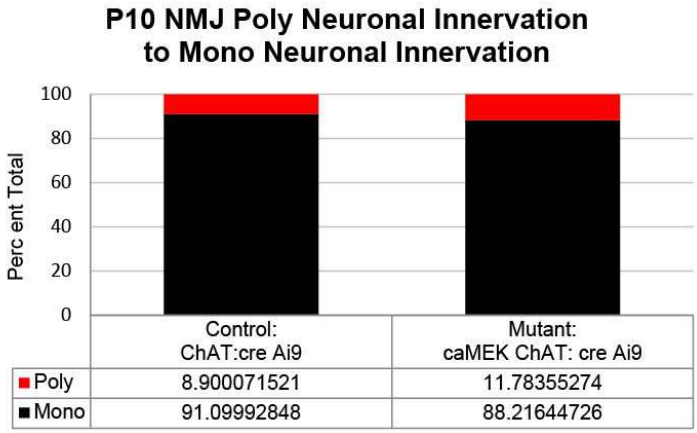

Figure 30: GOF P10 Poly-to-Mono Quantitative Analysis

Rotarod

To ascertain whether the Chat:cre, CaMEK$^{+/-}$, Ai9$^{+/-}$ mouse was able to coordinate its limbs and successfully perform a rigorous physical task we utilized the rotarod. For this behavioral assay we used 14 mutants and 10 age matched P60 controls (Figure 31). Though both groups showed statistically significant increases in the time they remained on the rotarod over the five-day period, there was no statistically significant difference between the two groups on day one (p= 0.202) or day five (p= 0.745) (Figure 32). The results of this behavioral assay show that an upregulation of Erk/MAPK doesn't affect the ability for the mice to balance and coordinate itself to perform this task.

	Control Average Latency	Control Standard Deviation	Mutant Average Latency	Mutant Standard Deviation
Day 1	78.15 seconds	27.48 seconds	65.67 seconds	19.14 seconds
Day 2	86.32 seconds	14.69 seconds	85.3 seconds	20.42 seconds
Day 3	114.85 seconds	34.16 seconds	96.02 seconds	17.30 seconds
Day 4	112.09 seconds	24.84 seconds	103.14 seconds	28.86 seconds
Day 5	130.18 seconds	26.44 seconds	126.95 seconds	21.63 seconds

Figure 31: GOF Rotarod Data

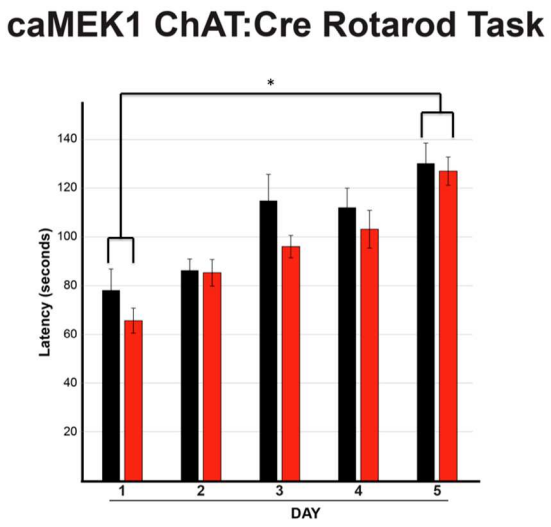

Figure 32: GOF Rotarod

Open Field

To ascertain whether the Chat:cre, CaMEK$^{+/-}$, Ai9$^{+/-}$ mouse had any detectable gross motor defects we utilized the open field behavioral paradigm. For this behavioral assay we used 12 mutants and 13 age matched controls ranging from ages P60-P180. Over a period of five minutes there was no statistically significant difference between total distance travelled ($p= 0.953$) or rate of travel ($p= 0.746$) between the two groups (Figure 33). The results of this behavioral assay show that an upregulation of Erk/MAPK doesn't affect gross motor behavior.

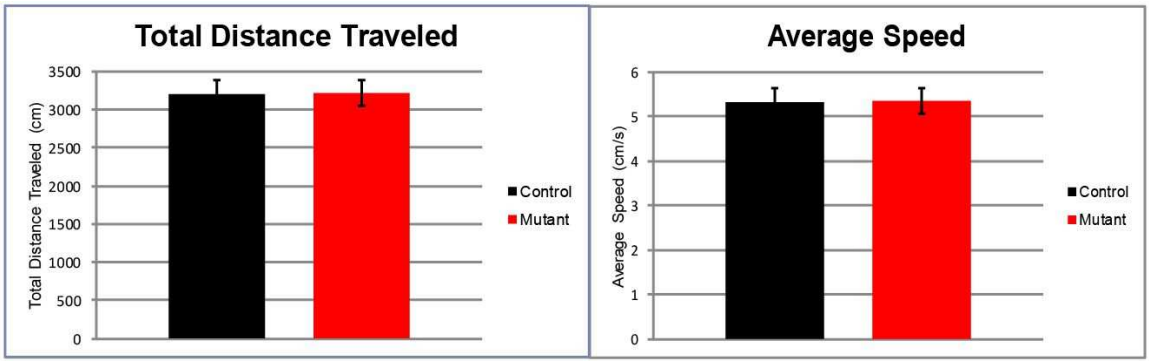

Figure 33: GOF Open Field

Weighted Object Test

To ascertain whether the Chat:cre, CaMEK$^{+/-}$, Ai9$^{+/-}$ mouse had problems with forelimb strength we utilized a weighted object test. For this behavioral assay we used 12 mutants and 9 age matched controls ranging from ages P80-P240. There was no statistically significant difference between the amounts of weight the two groups could hold (p= 0.532) (Figure 34). Thus it appears that an upregulation of Erk/MAPK doesn't affect the mouse's strength in this context.

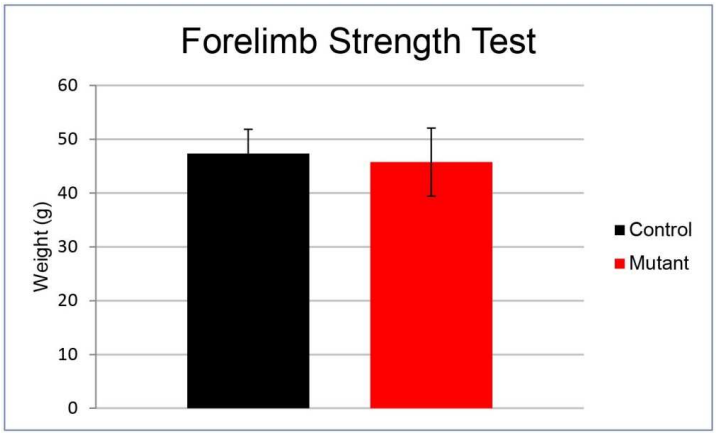

Figure 34: GOF Forelimb Test

Morris Water Maze

To ascertain whether the Chat:cre, CaMEK$^{+/-}$, Ai9$^{+/-}$ mouse had any detectable spatial memory deficits we utilized the Morris Water Maze. For this behavioral assay we used 12 mutants and 13 age matched controls ranging from ages P70-P230. Over a period of five days both groups took significantly less time to reach the reach the platform, however there was no statistically significant difference between the two groups performances on day one ($p= 0.48$) or day five ($p= 0.65$) (Figure 35). The results of this behavioral assay indicate that swim performance between the mutants and controls is intact and so is spatial memory acquisition and retrieval.

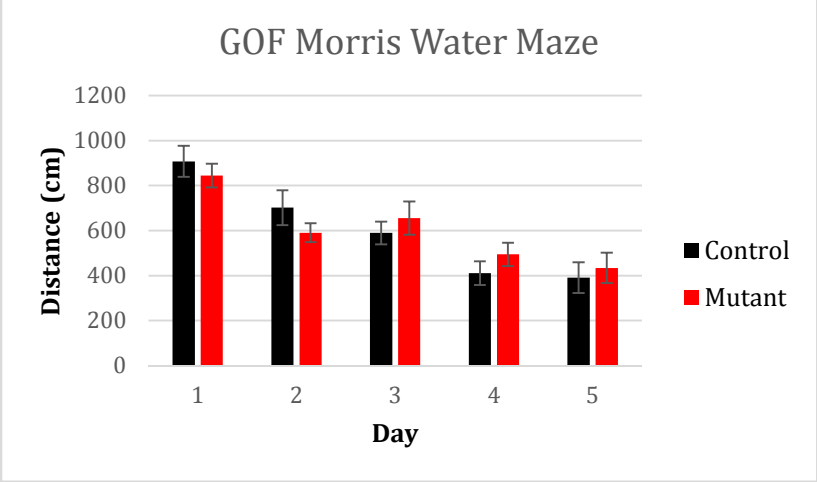

Figure 35: GOF Morris Water Maze

Rope Test

To ascertain whether the Chat:cre, CaMEK$^{+/-}$, Ai9$^{+/-}$ mouse had problems with forelimb strength we utilized a rope climbing assay. For this behavioral assay we used 9 mutants and 6 age matched controls ranging from ages P80-P240. The animals were habituated for one day. There was no statistically significant difference between the two groups performances on training day ($p= 0.146$) or testing day ($p= 0.105$) (Test day, Figure 36). Thus it appears that an upregulation of Erk/MAPK doesn't affect the mouse's strength in this context.

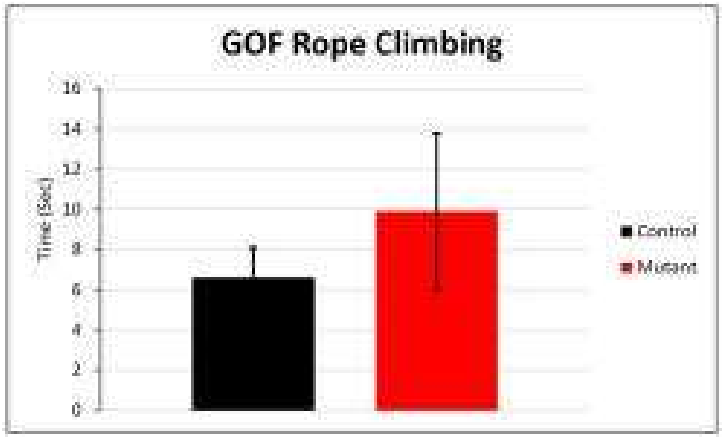

Figure 36: GOF Rope Climbing

CHAPTER V DISCUSSION

Previous work demonstrated that *embryonic* lower motor neuron survival, outgrowth, and NMJ formation is Erk1/2 independent (Newbern et al., 2011). We have assessed the functions of Erk1/2 in lower motor neurons during *postnatal* development. We have also assessed the effects of upregulating ERK/MAPK activity. The analysis has led to several conclusions. First, the loss of Erk/MAPK leads to a delay in NMJ morphological maturation, but left intact many other aspects of the postnatal development of lower motor neurons. Second, we found little evidence to suggest that the upregulation of ERK/MAPK activity has any effect on lower motor development.

Chat:Cre, Erk1/2, Loss-Of-Function Mouse Model

Newbern et al. 2011 investigated the role of Erk1/2 in motor neuron and oligodendrocyte development by utilizing Olig2:Cre directed recombination. The Olig2:Cre mouse induced recombination at E9.5 in ventral spinal cord progenitors that generate lower motor neurons and oligodendrocytes. Deficits in oligodendrocyte number were detected, however, since this mouse model died at birth, we were unable to study motor neuron development into the postnatal period. With the development of a mouse model that induces Cre recombination in lower motor neurons and lives past birth our research was aimed at addressing the role that Erk1/2 plays in the postnatal development of lower motor neurons.

Cell Survival in the Chat:cre, Erk1/2 LOF model

Motor neuron survival depends upon many different neurotrophins (Stifani, 2014). What these neurotrophins do and what signaling pathways they activate are well understood, but the precise functions of downstream signaling pathways are poorly defined. Previous research has shown that Erk1/2 signaling regulates cell survival in specific neuronal subtypes by promoting anti-apoptotic or pro-apoptotic transcription factors (Lu & Xu, 2006). Since motor neurons survive in the Chat:Cre LOF model we can conclude that lower motor neuron survival is Erk1/2 independent and is likely dependent upon other signaling pathways. One signaling pathway that could perhaps be more relevant for lower motor neuron survival is the PI3-kinase/Akt/mTOR pathway (Crowder & Freeman, 1998; Datta et al., 1997; Newbern et al., 2005; Philpott et al., 1997; Viewpoints, 1997). Previous research has shown that upregulated levels of mTOR activity protects against ALS induced motor neuron death (Saxena et al., 2013). Other research has shown cross talk between Erk1/2 and mTOR activity (Dai et al., 2014). Thus, it is possible that eliminating Erk1/2 signaling has no affect on lower motor neuron survival due to compensatory changes in mTOR or PI3-Kinase activity.

Activity-Dependent Mechanisms and Erk1/2 Signaling

Previous research has shown that glutamate receptor activation leads to high levels of phosphorylated Erk in several neuronal subtypes (Wang et al., 2007). Erk/MAPK is required for the insertion of new AMPA receptors into the dendritic spines of forebrain excitatory neurons during LTP and repeated depolarization of hippocampal

neurons induced the formation of new spines in an Erk/MAPK dependent manner (Lisman et al., 2001; Wu et al., 2001). Since activation of the Erk/MAPK pathway has been shown to be an integral part of activity dependent synaptic plasticity in many parts of the nervous system, we hypothesized Erk/MAPK is necessary for the activity-dependent morphological maturation of the lower motor neuron and the NMJ (Thomas & Huganir, 2004).

An examination of the electrophysiological properties of the lower motor neurons in the absence of Erk/MAPK would provide an important direct indicator of neuronal activity in mutant mice. However, the early lethality of LOF mice in the third postnatal week due to as yet unknown causes limited our ability to analyze this issue in detail. Overall, the mice exhibit growth delay and exhibit tremors. We cannot exclude that deficits in other cholinergic neurons, such as the sympathetic and parasympathetic neurons, could contribute to lethality. Nonetheless, our analysis of lower motor neurons demonstrates that Erk/MAPK is required for select developmental processes linked to activity, specifically, the morphological maturation of the NMJ into a 'pretzel'-like morphology. In contrast, other activity-dependent events, such as neuronal survival and the transition from mono-neuronal to poly-neuronal innervation were unaffected. Overall these data suggest the Erk/MAPK signaling mediates specific aspects of activity-dependent lower motor neuron development. Our work hints at the presence of distinct activity-dependent signaling mechanisms differentially linked to certain cellular processes. Further work will be necessary to identify the precise identity of these crucial molecular mediators.

Neuromuscular Junction Maturation in the Chat:Cre, Erk1/2 LOF Model

Previous research has shown that lower motor neuron synaptogenesis is Erk1/2 independent (Newbern et al., 2011). Subsequent maturation of the lower motor neuron NMJs in an Erk1/2 LOF model hasn't been studied. Our analysis led us to the conclusion that the proper morphological maturation of the NMJ is Erk1/2 dependent. NMJs in the LOF model fail to properly transition from plaque-to-pretzel morphology in the absence of Erk1/2. It is important to note that the ability of the postsynaptic membrane to mature occurs independent of any detectable defects in presynaptic morphology. Since our LOF model affected the lower motor neurons, not the muscle or surrounding Schwann cells, the failure for NMJs to properly mature could be linked to an inability to transduce the effects of growth cues from surrounding cells.

Signaling on The Presynaptic Membrane

FGF signaling has been shown to be crucial for the proper development of NMJs (Wu et al., 2010). It has also been shown that FGF signaling can recruit ERK/MAPK activity (Tsang & Dawid, 2004). These lines of reasoning lead us to hypothesize that our morphological phenotype may be caused by a disruption in FGF signaling. Previous research has shown that blocking FGF signaling at the NMJ causes a disruption in synaptic clustering at nerve terminals (Fox et al., 2007). Since our LOF model exhibits no noticeable issues with vesicle clustering at the NMJ we can conclude that the ability for FGF signaling to induce vesicular clustering is intact. This provides indirect evidence that FGF-dependent transport at the NMJ is Erk1/2 independent.

Another class of trans-synaptic signaling factors that play a major role in the proper maturation of the NMJ are the laminins (Wu et al., 2010). Previous research has shown that the two main receptor complexes that basal lamina proteins bind to, integrins and dystroglycans, activate Erk/MAPK signaling (Spence et al., 2004; X. Wu, 2008). Mice lacking laminin at the NMJ showed a disruption in presynaptic differentiation of the NMJ (Fox et al., 2007). Since our LOF mouse model exhibits no noticeable problem with presynaptic morphology, we conclude that laminins at the NMJ do not require Erk1/2 for the development of presynaptic morphology.

GDNF/RET signaling is another component that is necessary for the proper maturation of the NMJ (Wu et al., 2010). Past research has shown that GDNF activates two signaling pathways: the MAPK pathway and the PI3 kinase (Trupp et al., 1999). It is plausible that abolishing Erk1/2 activity in the motor neuron may affect the efficacy of GDNF signaling through RET. Previous research has shown that a loss of proper GDNF signaling at the NMJ causes two distinct phenotypes (Baudet et al., 2008). The first finding is that E18 embryos from RET knockout mutants exhibit developmentally delayed NMJs. The second finding is that adult NMJs from the Ret Nkx2.6:Cre model, which induces cre-mediated knockout of RET signaling in motor neurons, exhibit no structural abnormalities, but the total number of NMJs are reduced. Since the postnatal effects of RET deletion have not been studied it is unclear if they would exhibit a similar phenotype to that of the ChAT:$Cre^{+/-}$, $Erk1^{-\backslash-}$, $Erk2^{loxp/loxp}$, $Ai9^{+/-}$ mouse model. It is possible that in our LOF model that NMJs are developmentally delayed due to improper GDNF/RET signaling and that if the mice lived into adulthood that some of the

developmentally delayed NMJs would mature while others would atrophy.

Factors That Act on The Postsynaptic Membrane

It is possible that the NMJs aren't transitioning from plaque to pretzel due to a lack of a specific cue from the lower motor neuron. Previous research has shown that NMJs from mutant mice lacking ephexin1 fail to properly transition from plaque to pretzel (Shi et al., 2010). Ephexin1 is a downstream effector of EphA4 signaling which has been linked to actin cytoskeletal dynamics in the NMJ (Shi et al., 2010). Perhaps ephrin ligand expression is regulated by Erk1/2 activity in the lower motor neuron and could explain the morphological phenotype in our LOF model.

Agrin is arguably the most important mediator of NMJ development. It is seen as a master organizer of the NMJ and mice that lack agrin fail to form NMJs and AChRs fail to properly cluster (Gautam et al., 1996). Given that our Erk1/2 LOF model forms synapses, albeit developmentally delayed, it is unlikely that agrin could be the source of our phenotype. However, previous research by Bolliger et al. 2010 has shown that specific proteolytic cleavage of agrin acts as a crucial regulatory step in the maturation of the NMJ (Bolliger et al., 2010). Bolliger et al. 2010 found that cleavage-resistant agrin in motor neurons caused developmentally delayed NMJs that appear similar to the NMJs in our Erk1/2 LOF model. There are two possibilities that can explain this phenotype. The first is that in the absence of Erk1/2 motor neurons are unable to produce a specific protease that can cleave agrin. Which specific protease that may be is unclear. Bolliger et al. ruled out the possibility of neurotrypsin and MMP-3 as candidate proteases since NMJ

maturation occurs at a normal rate in the absence of these proteins. The second possibility is that Erk1/2 somehow mediate the cleavage of agrin itself.

Chat:cre, CAMEK Gain-Of-Function Mouse Model

Given the fact that the majority of the Rasopathies are caused by GOF mutations, it is crucial that we understand how upregulation of Erk/MAPK activity affects individual cell types (Rauen, 2013). Past research has shown that patients with Rasopathies frequently possess muscular defects (D. A. Stevenson & Yang, 2011). Much of the research conducted on this subject has only investigated the role of Rasopathy mutations in the muscle itself, but not the motor neuron. Our research aimed to address whether an upregulation of Erk/MAPK activity in the lower motor neuron had any adverse affects on the proper development of the lower motor neuron.

Cell survival and Activity in the Chat:Cre, CAMEK GOF Model

Just like the LOF model, the GOF model exhibited normal lower motor neuron survival. Also, just like the LOF model preliminary evidence suggests that levels of phosphorylated CREB are normal as well (not shown). Even though there is much evidence to support that Erk/MAPK plays an important role in activity dependent gene regulation and synaptic plasticity in other neuronal subtypes, it's possible the that lower motor neurons don't rely upon Erk/MAPK as heavily to accomplish these mechanisms. However, it's also possible that phosphatases are able to detect an increase in Erk/MAPK activity and attenuate the high level signaling (Kondoh & Nishida, 2007). This prospect

seems more viable considering the phenotype we observed in the Erk1/2 LOF model. We hypothesized that the developmental delay observed in the Erk1/2 LOF model is due to a decrease in neuronal activity due to a downregulation of Erk-mediated AMPAR insertion in the lower motor neuron's dendritic spines. If lower motor neurons truly do utilize Erk/MAPK signaling for activity-dependent gene regulation and synaptic plasticity, one would hypothesize that an unbalanced increase in Erk/MAPK signaling would lead to an increase in neuronal activity due to an upregulation of Erk-mediated AMPAR insertion in the lower motor neuron's dendritic spines. The result of an increase in activity would be apparent in the process of NMJ maturation and axonal pruning. Since we didn't observe acceleration in either of these processes it is possible that either phosphates regulate the increase in Erk/MAPK activity or the lower motor neuron doesn't heavily rely upon Erk/MAPK signaling.

NMJ Maturation in the Chat:Cre, CAMEK GOF Model

Unlike the NMJs of the LOF model, the NMJs of the GOF model exhibit no obvious delays in maturation. The NMJs transition from plaque-to-pretzel at a normal rate, transition from poly-neuronal innervation to mono-neuronal innervation, and the morphology of both the presynaptic and postsynaptic aspect of the NMJ appear normal. Thus we can conclude that upregulating Erk/MAPK activity doesn't affect the proper morphological maturation of the NMJ or the temporal dynamics of its activity-dependent maturation.

Behavioral Testing of the Chat:Cre, CAMEK GOF Model

Our analysis of the GOF mouse model led us to the conclusion that lower motor neuron development is unaffected by an upregulation of Erk/MAPK activity. This was a puzzling finding given the fact that we observed mild aberrant limb positioning in this mouse model. Since this phenotype couldn't be explained by our histological analyses we executed several behavioral tests to more rigorously define this phenotype.

The open field, rotarod, rope-climbing, and strength tests all resulted in negative findings. The behavioral assays showed no change in gross motor behavior, coordination, or strength. Since these findings produced no explanation for the mild behavioral phenotypes we observed in this mouse model, we decided to test for another aspect of behavior, spatial memory.

The Chat:cre CAMEK GOF model targets not only cholinergic lower motor neurons in the spinal cord, but also cholinergic neurons of the basal forebrain (Zaborszky et al., 2012). These cholinergic neurons play an distinct role in spatial memory (Okada et al., 2014). Preliminary evidence showed that in the GOF model these cholinergic neurons are intact (data not shown). Since this population of neurons was intact we predicted that there would be no difference in performance compared to litter mate controls in the watermaze behavioral assay. We found that the mice performed just as well as their age-matched controls in spatial memory acquisition. Thus we can conclude that upregulating Erk/MAPK activity has no noticeable effect on spatial memory formation.

CHAPTER VI CONCLUSION

Many Rasopathy patients exhibit abnormal muscular defects including hypotonia, decreased motor proficiency, decreased strength, variable muscle fiber size, and myopathy (Stevenson et al., 2012). Previous research has shown that these mutations arise from Erk/MAPK mutations in the muscle fibers. Whether these mutations can also arise from Erk/MAPK mutations in the motor neurons as well was unclear until now. The Erk1/2 GOF model that we generated exhibited normal lower motor neuron development and didn't phenocopy any of the typical Rasopathy muscular deficits. We concluded that GOF Erk/MAPK mutations in the lower motor neurons are unlikely to cause the muscular abnormalities typically found in Rasopathy patients. However, the delay in morphological maturation observed in the NMJs of the LOF Erk/MAPK mouse model indicates some role of Erk/MAPK for the proper postnatal maturation of lower motor neurons. Further research needs to be done to elucidate how exactly Erk/MAPK activity regulates the proper postnatal development of the lower motor neuron. This research may provide valuable insight into why some neurons rely more heavily upon Erk/MAPK signaling than others. By elucidating how some neurons bypass the need for Erk/MAPK signaling, or rely less heavily upon it, we may be able to understand how to implement better treatment strategies for those who suffer from the neurological symptoms that arise from the neurons affected by Erk/MAPK mutations in Rasopathy patients.

REFERENCES

Banks, G. B. (2005). Glycinergic and GABAergic Synaptic Activity Differentially Regulate Motoneuron Survival and Skeletal Muscle Innervation. *Journal of Neuroscience*, *25*(5), 1249–1259. http://doi.org/10.1523/JNEUROSCI.1786-04.2005

Barry, J. a, & Ribchester, R. R. (1995). Persistent polyneuronal innervation in partially denervated rat muscle after reinnervation and recovery from prolonged nerve conduction block. *The Journal of Neuroscience*, *15*(10), 6327–39. Retrieved from http://www.ncbi.nlm.nih.gov/pubmed/7472398

Baudet, C., Pozas, E., Adameyko, I., Andersson, E., Ericson, J., & Ernfors, P. (2008). Retrograde Signaling onto Ret during Motor Nerve Terminal Maturation. *Journal of Neuroscience*, *28*(4), 963–975. http://doi.org/10.1523/JNEUROSCI.4489-07.2008

Bessou, P., Emonet-Denand, F., & Laporte, Y. (1965). Motor fibres innervating extrafusal and intrafusal muscle fibres in the cat. *Journal of Physiology*, *180*(3), 649–672. http://doi.org/10.1113/jphysiol.1965.sp007722

Bevan, S., & Steinbach, J. H. (1977). The distribution of alpha-bungarotoxin binding sites of mammalian skeletal muscle developing in vivo. *The Journal of Physiology*, *267*(1), 195–213. http://doi.org/10.1113/jphysiol.1977.sp011808

Bolliger, M. F., Zurlinden, A., Lüscher, D., Bütikofer, L., Shakhova, O., Francolini, M., … Sonderegger, P. (2010). Specific proteolytic cleavage of agrin regulates maturation of the neuromuscular junction. *Journal of Cell Science*, *123*(Pt 22), 3944–3955. http://doi.org/10.1242/jcs.072090

Bolshakov, V. Y., Carboni, L., Cobb, M. H., Siegelbaum, S. A., & Belardetti, F. (2000). Dual MAP kinase pathways mediate opposing forms of long-term plasticity at CA3 – CA1 synapses, 1107–1112.

Brandon, E. P., Lin, W., Amour, K. A. D., Pizzo, D. P., Dominguez, B., Sugiura, Y., … Lee, K. (2003). Aberrant Patterning of Neuromuscular Synapses in Choline Acetyltransferase-Deficient Mice, *23*(2), 539–549.

Briscoe, J., & Ericson, J. (2001). Specification of neuronal fates in the ventral neural tube. *Current Opinion in Neurobiology*, *11*(1), 43–49. http://doi.org/10.1016/S0959-4388(00)00172-0

Buckingham, M., Bajard, L., Chang, T., Daubas, P., Hadchouel, J., Meilhac, S., … Relaix, F. (2003). The formation of skeletal muscle: From somite to limb. *Journal of Anatomy*, *202*(1), 59–68. http://doi.org/10.1046/j.1469-7580.2003.00139.x

Buffelli, M., Burgess, R. W., Feng, G., Lobe, C. G., Lichtman, J. W., & Sanes, J. R. (2003). Genetic evidence that relative synaptic efficacy biases the outcome of synaptic competition. *Nature*, *424*(6947), 430–434. http://doi.org/10.1038/nature01836.1.

Burke, R. E., Levine, D. N., Tsairis, P., & Zajac III, F. E. (1973). Physiological types and histochemical profiles in motor units of the cat gastrocnemius. *The Journal of Physiology*, *234*(3), 723–748. http://doi.org/10.1113/jphysiol.1973.sp010369

Colman, A. H., Nabekura, J., & Lichtman, J. W. (1997). Alterations in Synaptic Strength Preceding Axon Withdrawal Published by : American Association for the Advancement of Science Alterations in Synaptic Strength Preceding Axon Withdrawal, *275*(5298), 356–361.

Crowder, R. J., & Freeman, R. S. (1998). Phosphatidylinositol 3-Kinase and Akt Protein Kinase Are Necessary and Sufficient for the Survival of Nerve Growth Factor-Dependent Sympathetic Neurons, *18*(8), 2933–2943.

Dai, J., Bercury, K. K., & Macklin, W. B. (2014). Interaction of mTOR and Erk1/2 signaling to regulate oligodendrocyte differentiation. *Glia*, *62*(12), 2096–2109. http://doi.org/10.1002/glia.22729

Dai, Z., Luo, X., Xie, H., & Peng, H. B. (2000). The actin-driven movement and formation of acetylcholine receptor clusters. *Journal of Cell Biology*, *150*(6), 1321–1334. http://doi.org/10.1083/jcb.150.6.1321

Darabid, H., Perez-Gonzalez, A. P., & Robitaille, R. (2014). Neuromuscular synaptogenesis: coordinating partners with multiple functions. *Nature Reviews Neuroscience*, (October), 1–16. http://doi.org/10.1038/nrn3821

Dasen, J. S., & Jessell, T. M. (2009). *Chapter Six Hox Networks and the Origins of Motor Neuron Diversity*. *Current Topics in Developmental Biology* (1st ed., Vol. 88). Elsevier Inc. http://doi.org/10.1016/S0070-2153(09)88006-X

Dasen, J. S., Tice, B. C., Brenner-Morton, S., & Jessell, T. M. (2005). A Hox regulatory network establishes motor neuron pool identity and target-muscle connectivity. *Cell*, *123*(3), 477–491. http://doi.org/10.1016/j.cell.2005.09.009

Datta, S. R., Dudek, H., Tao, X., Masters, S., Fu, H., Gotoh, Y., & Greenberg, M. E. (1997). Akt Phosphorylation of BAD Couples Survival Signals to the Cell-Intrinsic Death Machinery, *91*, 231–241.

DeChiara, T. M., Bowen, D. C., Valenzuela, D. M., Simmons, M. V, Poueymirou, W. T., Thomas, S., … Yancopoulos, G. D. (1996). The receptor tyrosine kinase MuSK is required for neuromuscular junction formation in vivo. *Cell*, *85*(4), 501–512.

http://doi.org/10.1016/S0092-8674(00)81251-9

Del Castillo, J., & Katz, B. (1954). Quantal Components of the End-Plate Potential. *J. Physiol*, *124*, 560–573. http://doi.org/10.1016/j.neuron.2009.06.014

Eftimie, R., Brenner, H. R., & Buonanno, A. (1991). Myogenin and MyoD join a family of skeletal muscle genes regulated by electrical activity. *Proc Natl Acad Sci U S A*, *88*(4), 1349–1353. http://doi.org/10.1073/pnas.88.4.1349

Finn, A. J., Feng, G., & Pendergast, A. M. (2003). Postsynaptic requirement for Abl kinases in assembly of the neuromuscular junction. *Nat Neurosci*, *6*(7), 717–723. http://doi.org/10.1038/nn1071

Flucher, B. E., & Daniels, M. P. (1989). Distribution of Na+ channels and ankyrin in neuromuscular junctions is complementary to that of acetylcholine receptors and the 43 kd protein. *Neuron*, *3*(2), 163–175. http://doi.org/10.1016/0896-6273(89)90029-9

Fox, M. A., Sanes, J. R., Borza, D. B., Eswarakumar, V. P., F??ssler, R., Hudson, B. G., … Umemori, H. (2007). Distinct Target-Derived Signals Organize Formation, Maturation, and Maintenance of Motor Nerve Terminals. *Cell*, *129*(1), 179–193. http://doi.org/10.1016/j.cell.2007.02.035

Gallarda, B. W., Bonanomi, D., Muller, D., Brown, A., Alaynick, W. A., Andrews, S. E., … Marquardt, T. (2008). Segregation of Axial Motor and Sensory Pathways via Heterotypic Trans-Axonal Signaling. *Science (New York, N.Y.)*, *320*(5873), 233–6. http://doi.org/10.1126/science.1153758

Gautam, M., Noakes, P. G., Moscoso, L., Rupp, F., Scheller, R. H., Merlie, J. P., & Sanes, J. R. (1996). Defective neuromuscular synaptogenesis in agrin-deficient mutant mice. *Cell*, *85*(4), 525–535. http://doi.org/10.1016/S0092-8674(00)81253-2

Gesemann, M., Denzer, A. J., & Ruegg, M. A. (1995). Acetylcholine receptor-aggregating activity of agrin isoforms and mapping of the active site. *Journal of Cell Biology*, *128*(4), 625–636. http://doi.org/10.1083/jcb.128.4.625

Glass, D. J., Bowen, D. C., Stitt, T. N., Radziejewski, C., Bruno, J. A., Ryan, T. E., … Yancopoulos, G. D. (1996). Agrin acts via a MuSK receptor complex. *Cell*, *85*(4), 513–523. http://doi.org/10.1016/S0092-8674(00)81252-0

Ikonomidou, C. (1999). Blockade of NMDA Receptors and Apoptotic Neurodegeneration in the Developing Brain. *Science*, *283*(5398), 70–74. http://doi.org/10.1126/science.283.5398.70

Johnson, B., Macwilliams, B., Carey, J. C., David, H., Astous, J. L. D., & Stevenson, D. A. (2011). Motor Proficiency in Children with Neurofibromatosis Type 1. *Pediatri*

Phys Ther, *22*(4), 344–348. http://doi.org/10.1097/PEP.0b013e3181f9dbc8.

Kim, N., & Burden, S. J. (2008). MuSK controls where motor axons grow and form synapses. *Nature Neuroscience*, *11*(1), 19–27. http://doi.org/10.1038/nn2026

Krenz, M., Gulick, J., Osinka, H., Colbert, M., Moltentin, J., & Robbins, J. (2008) Role of Erk1/2 in congenital valve malformations in Noonan syndrome. *PNAS*, 105(48) 18390-18935

Kondoh, K., & Nishida, E. (2007). Regulation of MAP kinases by MAP kinase phosphatases. *Biochimica et Biophysica Acta - Molecular Cell Research*, *1773*(8), 1227–1237. http://doi.org/10.1016/j.bbamcr.2006.12.002

Lappin, T. R. J., Grier, D. G., Thompson, A., & Halliday, H. L. (2006). HOX genes: Seductive science, mysterious mechanisms. *Ulster Medical Journal*, *75*(1), 23–31.

Lee, C. W., Han, J., Bamburg, J. R., Han, L., Lynn, R., & Zheng, J. Q. (2009). Regulation of acetylcholine receptor clustering by ADF/cofilin-directed vesicular trafficking. *Nature Neuroscience*, *12*(7), 848–856. http://doi.org/10.1038/nn.2322

Lisman, J., Schulman, H., & Cline, H. (2002). THE MOLECULAR BASIS OF CaMKII FUNCTION IN SYNAPTIC AND BEHAVIOURAL MEMORY, *3*(March).

Liu, A., & Niswander, L. A. (2005). Bone morphogenetic protein signalling and vertebrate nervous system development. *Nature Reviews. Neuroscience*, *6*(12), 945–54. http://doi.org/10.1038/nrn1805

Liu, J.-P., Laufer, E., & Jessell, T. M. (2001). Assigning the Positional Identity of Spinal Motor Neurons. *Neuron*, *32*(6), 997–1012. http://doi.org/10.1016/S0896-6273(01)00544-X

Lu, Z., & Xu, S. (2006). ERK1/2 MAP kinases in cell survival and apoptosis. *IUBMB Life (International Union of Biochemistry and Molecular Biology: Life)*, *58*(11), 621–631. http://doi.org/10.1080/15216540600957438

Luo, Z. G., Je, H. S., Wang, Q., Yang, F., Dobbins, G. C., Yang, Z. H., … Mei, L. (2003). Implication of geranylgeranyltransferase I in synapse formation. *Neuron*, *40*(4), 703–717. http://doi.org/10.1016/S0896-6273(03)00695-0

Luo, Z. G., Wang, Q., Zhou, J. Z., Wang, J., Luo, Z., Liu, M., … Mei, L. (2002). Regulation of AChR clustering by Dishevelled interacting with MuSK and PAK1. *Neuron*, *35*(3), 489–505. http://doi.org/10.1016/S0896-6273(02)00783-3

Madisen, L., Zwingman, T. A., Sunkin, S. M., Oh, S. W., Zariwala, H. A., Gu, H., … Zeng, H. (2010). A robust and high-throughput Cre reporting and characterization

system for the whole mouse brain. *Nat Neurosci*, *13*(1), 133–140

Mendell, L. M. (2005). The size principle: a rule describing the recruitment of motoneurons. *J Neurophysiol*, *93*(6), 3024–3026. http://doi.org/10.1152/classicessays.00025.2005

Newbern, J. M., Li, X., Shoemaker, S. E., Zhou, J., Zhong, J., Wu, Y., … Snider, W. D. (2011). Specific functions for ERK/MAPK signaling during PNS development. *Neuron*, *69*(1), 91–105. http://doi.org/10.1016/j.neuron.2010.12.003

Okada, K. (2006). The Muscle Protein Dok-7 Is Essential for Neuromuscular Synaptogenesis. *Science*, *312*(5781), 1802–1805. http://doi.org/10.1126/science.1127142

Okada, K., Nishizawa, K., Kobayashi, T., Sakata, S., & Kobayashi, K. (2014). Distinct roles of basal forebrain cholinergic neurons in spatial and object recognition memory. *Nature Publishing Group*, 1–13. http://doi.org/10.1038/srep13158

Oppenheim. (1991). Cell death during development of the nervous system, 453–501.

Philpott, K. L., Mccarthy, M. J., Klippel, A., & Rubin, L. L. (1997). Activated Phosphatidylinositol 3-Kinase and Akt Kinase Promote Survival of Superior Cervical Neurons, *139*(3), 809–815.

Pittman, R. H., & Oppenheim, R. W. (1978). Neuromuscular blockade increases motoneurone survival during normal cell death in the chick embryo. *Nature*. http://doi.org/10.1038/271364a0

Rauen, K. A. (2013). The RASopathies. *Annu Rev Genomics Hum Genet*, *14*, 355–369. http://doi.org/10.1146/annurev-genom-091212-153523

Rossi, J., Balthasar, N., Olson, D., Scott, M., Berglund, E., Lee, C., Choi, M., Lauzon, D., Lowell, B., & Elmquist, J. (2011) Melanocortin-4-receptors Expressed by Cholinergic Neurons Regulate Energy Balance and Glucose Homeostasis. *Cell Metabolism*, 13(2), 195-204

Saba-el-leil, M. K., Ang, S., Le, K., Saba-el-leil, M. K., Le, K., Ang, S., & Meloche, S. (2015). Functional Redundancy of ERK1 and ERK2 MAP Kinases during Development Report Functional Redundancy of ERK1 and ERK2 MAP Kinases during Development, 913–921. http://doi.org/10.1016/j.celrep.2015.07.011

Salpeter, M. M., & Loring, R. H. (1985). Nicotinic acetylcholine receptors in vertebrate muscle: Properties, distribution and neural control. *Progress in Neurobiology*, *25*(4), 297–325. http://doi.org/10.1016/0301-0082(85)90018-8

Samuels, I., Karlo, C., Faruzzi, A., Pickering, K., Herrup, K., & Sweatt, D., Saitta, S., and Landreth, G. (2008). Deletion of ERK2 Mitogen-Activated Protein Kinase Identifies Its Key Roles in Cortical Neurogenesis and Cognitive Function (2008) *J. Neuroscience*, *28*(27), 6983–6995. http://doi.org/10.1038/nature13478

Sanes, J. R., & Lichtman, J. W. (1999). Development of the vertebrate neuromuscular junction. *Annual Review of Neuroscience*, *22*, 389–442. http://doi.org/10.1146/annurev.neuro.22.1.389

Saxena, S., Roselli, F., Singh, K., Leptien, K., Julien, J. P., Gros-Louis, F., & Caroni, P. (2013). Neuroprotection through Excitability and mTOR Required in ALS Motoneurons to Delay Disease and Extend Survival. *Neuron*, *80*(1), 80–96. http://doi.org/10.1016/j.neuron.2013.07.027

Shi, L., Butt, B., Ip, F. C. F., Dai, Y., Jiang, L., Yung, W. H., … Ip, N. Y. (2010). Ephexin1 Is Required for Structural Maturation and Neurotransmission at the Neuromuscular Junction. *Neuron*, *65*(2), 204–216. http://doi.org/10.1016/j.neuron.2010.01.012

Shirasaki, R., Lewcock, J. W., Lettieri, K., & Pfaff, S. L. (2006). FGF as a Target-Derived Chemoattractant for Developing Motor Axons Genetically Programmed by the LIM Code. *Neuron*, *50*(6), 841–853. http://doi.org/10.1016/j.neuron.2006.04.030

Souza, J. F., Passos, R. L. F., Guedes, A. C. M., Rezende, N. A., & Rodrigues, L. O. C. (2009). Muscular force is reduced in neurofibromatosis type 1. *Journal of Musculoskeletal Neuronal Interactions*, *9*(1), 15–17.

Spence, H. J., Dhillon, A. S., James, M., & Winder, S. J. (2004). Dystroglycan, a scaffold for the ERK–MAP kinase cascade. *EMBO Reports*, *5*(5), 484–489. http://doi.org/10.1038/sj.embor.7400140

Stevenson, D. A., & Yang, F. C. (2011). The musculoskeletal phenotype of the RASopathies. *American Journal of Medical Genetics, Part C: Seminars in Medical Genetics*, *157*(2), 90–103. http://doi.org/10.1002/ajmg.c.30296

Stevenson, D. a, Moyer-Mileur, L. J., Carey, J. C., Quick, J. L., Hoff, C. J., & Viskochil, D. H. (2005). Case-control study of the muscular compartments and osseous strength in neurofibromatosis type 1 using peripheral quantitative computed tomography. *Journal of Musculoskeletal & Neuronal Interactions*, *5*(2), 145–9. Retrieved from http://www.ncbi.nlm.nih.gov/pubmed/15951630

Stifani, N. (2014). Motor neurons and the generation of spinal motor neuron diversity. *Frontiers in Cellular Neuroscience*, *8*(October), 293. http://doi.org/10.3389/fncel.2014.00293

Tessier-Lavigne, M., & Goodman, C. (1996). The Molecular Biology of Axon Guidance. *Science*, *274*(5290), 1123–1133. http://doi.org/10.1126/science.274.5290.1123

Thomas, G. M., & Huganir, R. L. (2004). MAPK CASCADE SIGNALLING AND synapotic plasticity , *5*(March). http://doi.org/10.1038/nrn1346

Tidyman, W. E., Lee, H. S., & Rauen, K. A. (2011). Skeletal muscle pathology in Costello and cardio-facio-cutaneous syndromes: Developmental consequences of germline Ras/MAPK activation on myogenesis. *American Journal of Medical Genetics, Part C: Seminars in Medical Genetics*, *157*(2), 104–114. http://doi.org/10.1002/ajmg.c.30298

Trupp, M., Scott, R., Whittemore, S. R., & Ibanez, C. F. (1999). Ret-dependent and - independent mechanisms of glial cell line-derived neurotrophic factor signaling in neuronal cells. *Journal of Biological Chemistry*, *274*(30), 20885–20894. http://doi.org/10.1074/jbc.274.30.20885

Tsang, M., & Dawid, I. B. (2004). Promotion and attenuation of FGF signaling through the Ras-MAPK pathway. *Science's STKE : Signal Transduction Knowledge Environment*, *2004*(228), pe17. http://doi.org/10.1126/stke.2282004pe17

van der Burgt, I., Kupsky, W., Stassou, S., Nadroo, A., Barroso, C., Diem, A., … Zenker, M. (2007). Myopathy caused by HRAS germline mutations: implications for disturbed myogenic differentiation in the presence of constitutive HRas activation. *Journal of Medical Genetics*, *44*(7), 459–62. http://doi.org/10.1136/jmg.2007.049270

Viewpoints, F. O. (1997). Regulation of neuronal survival by the serine- threonine protein kinase Akt, (12).

Viskochil, D. H., Ph, D., Astous, J. L. D., & David, A. (2013). Lower Extremity Strength and Hopping and Jumping Ground Reaction forces in Children with Neurofibromatosis Type 1, *31*(1), 247–254. http://doi.org/10.1016/j.humov.2011.05.004.

Wang, J. Q., Fibuch, E. E., & Mao, L. (2007). Regulation of mitogen-activated protein kinases by glutamate receptors. *Journal of Neurochemistry*, *100*(1), 1–11. http://doi.org/10.1111/j.1471-4159.2006.04208.x

Weatherbee, S. D., Anderson, K. V., & Niswander, L. A. (2006). LDL-receptor-related protein 4 is crucial for formation of the neuromuscular junction. *Development*, *133*(24), 4993–5000. http://doi.org/10.1242/dev.02696

Webb, B. A., Zhou, S., Eves, R., Shen, L., Jia, L., & Mak, A. S. (2006). Phosphorylation of cortactin by p21-activated kinase. *Archives of Biochemistry and Biophysics*,

456(2), 183–193. http://doi.org/10.1016/j.abb.2006.06.011

Weston, C., Gordon, C., Teressa, G., Hod, E., Ren, X. D., & Prives, J. (2003). Cooperative regulation by Rac and Rho of agrin-induced acetylcholine receptor clustering in muscle cells. *Journal of Biological Chemistry*, *278*(8), 6450–6455. http://doi.org/10.1074/jbc.M210249200

Woodhoo, A., & Sommer, L. (2008). Development of the schwann cell lineage: From the neural crest to the myelinated nerve. *Glia*, *56*(14), 1481–1490. http://doi.org/10.1002/glia.20723

Wu, G., Deisseroth, K., & Tsien, R. W. (2001). Spaced stimuli stabilize MAPK pathway activation and its effects on dendritic morphology.

Wu, H., Xiong, W. C., & Mei, L. (2010). To build a synapse: signaling pathways in neuromuscular junction assembly. *Development*, *137*(7), 1017–1033. http://doi.org/10.1242/dev.038711

Wu, H., Xiong, W. C., & Mei, L. (2010). To build a synapse: signaling pathways in neuromuscular junction assembly. *Development*, *137*(7), 1017–33. http://doi.org/10.1242/dev.038711

Wu, X. (2008). Integrins as Receptor Targets for Neurological Disorders. *Nano*, *6*(9), 2166–2171. http://doi.org/10.1021/nl061786n

Yang, X., Arber, S., William, C., Li, L., Tanabe, Y., Jessell, T. M., … Burden, S. J. (2001). Patterning of muscle acetylcholine receptor gene expression in the absence of motor innervation. *Neuron*, *30*(2), 399–410. http://doi.org/10.1016/S0896-6273(01)00287-2

Zaborszky, L., Pol, A. Van Den, & Gyengesi, E. (2012). *The Basal Forebrain Cholinergic Projection System in Mice*. http://doi.org/10.1016/B978-0-12-369497-3.10028-7

Zhang, B., Luo, S., Wang, Q., Suzuki, T., Xiong, W. C., & Mei, L. (2008). LRP4 Serves as a Coreceptor of Agrin. *Neuron*, *60*(2), 285–297. http://doi.org/10.1016/j.neuron.2008.10.006

Zhu, D., Yang, Z., Luo, Z., Luo, S., Xiong, W. C., & Mei, L. (2008). Muscle-Specific Receptor Tyrosine Kinase Endocytosis in Acetylcholine Receptor Clustering in Response to Agrin. *Journal of Neuroscience*, *28*(7), 1688–1696. http://doi.org/10.1523/JNEUROSCI.4130-07.2008